



HAL
open science

Insight into the wheat residues-derived adsorbents for the remediation of organic and inorganic aquatic contaminants: A review

Muthanna J. Ahmed, Ioannis Anastopoulos, Dimitrios Kalderis, Muhammad Haris Mahyuddin, Muhammad Usman

► To cite this version:

Muthanna J. Ahmed, Ioannis Anastopoulos, Dimitrios Kalderis, Muhammad Haris Mahyuddin, Muhammad Usman. Insight into the wheat residues-derived adsorbents for the remediation of organic and inorganic aquatic contaminants: A review. *Environmental Research*, 2024, 250, pp.118507. 10.1016/j.envres.2024.118507 . hal-04479258

HAL Id: hal-04479258

<https://hal.science/hal-04479258v1>

Submitted on 29 May 2024

HAL is a multi-disciplinary open access archive for the deposit and dissemination of scientific research documents, whether they are published or not. The documents may come from teaching and research institutions in France or abroad, or from public or private research centers.

L'archive ouverte pluridisciplinaire **HAL**, est destinée au dépôt et à la diffusion de documents scientifiques de niveau recherche, publiés ou non, émanant des établissements d'enseignement et de recherche français ou étrangers, des laboratoires publics ou privés.



Distributed under a Creative Commons Attribution - NonCommercial 4.0 International License

Journal Pre-proof

Insight into the wheat residues-derived adsorbents for the remediation of organic and inorganic aquatic contaminants: A review

Muthanna J. Ahmed, Ioannis Anastopoulos, Dimitrios Kalderis, Muhammad Haris, Muhammad Usman

PII: S0013-9351(24)00411-0

DOI: <https://doi.org/10.1016/j.envres.2024.118507>

Reference: YENRS 118507

To appear in: *Environmental Research*

Received Date: 8 December 2023

Revised Date: 9 February 2024

Accepted Date: 15 February 2024

Please cite this article as: Ahmed, M.J., Anastopoulos, I., Kalderis, D., Haris, M., Usman, M., Insight into the wheat residues-derived adsorbents for the remediation of organic and inorganic aquatic contaminants: A review, *Environmental Research* (2024), doi: <https://doi.org/10.1016/j.envres.2024.118507>.

This is a PDF file of an article that has undergone enhancements after acceptance, such as the addition of a cover page and metadata, and formatting for readability, but it is not yet the definitive version of record. This version will undergo additional copyediting, typesetting and review before it is published in its final form, but we are providing this version to give early visibility of the article. Please note that, during the production process, errors may be discovered which could affect the content, and all legal disclaimers that apply to the journal pertain.



1 **Insight into the wheat residues-derived adsorbents for the remediation of organic and**
2 **inorganic aquatic contaminants: A review**

3
4 Muthanna J. Ahmed^{a*}, Ioannis Anastopoulos^b, Dimitrios Kalderis^c, Muhammad Haris^d,
5 Muhammad Usman^e

6
7 ^aDepartment of Chemical Engineering, College of Engineering, University of Baghdad, 10071
8 Baghdad, Iraq

9 ^bDepartment of Agriculture, University of Ioannina, UoI Kostakii Campus, 47040 Arta, Greece

10 ^cLaboratory of Environmental Technologies and Applications, Department of Electronic
11 Engineering, Hellenic Mediterranean University, Chania 73100, Greece

12 ^dSchool of Environmental Science and Engineering, Shaanxi University of Science &
13 Technology, Xi'an 710021, P.R. China.

14 ^eUniversité de Rennes, École Nationale Supérieure de Chimie de Rennes, CNRS, UMR 6226, F-
15 35000, Rennes, France.

16
17 * Corresponding author. Tel.: +9647801642643

18 E-mail address: muthanna.ja@gmail.com (Muthanna J. Ahmed)

Abstract

Wheat is a major grain crop of the world that provides a stable food for human consumption. Large amounts of by-products /waste materials are produced after the harvesting and processing of wheat crop. Such materials can cause an environmental issue if not disposed of properly. Several studies have shown that wheat residues can be efficient precursors for adsorbents because of their availability, renewability, lignocellulosic composition, and surface active groups enriched structure. In the literature, there are few review articles that address wheat residues-based adsorbents. For instance, the use of raw wheat straw and bran as adsorbents for heavy metals and wheat bran-based adsorbents against dyes. However, these reviews were specific in terms of adsorbate or adsorbent and did not provide detailed information about the modification, properties, and regeneration of these adsorbents. This article extensively reviews the utilization of wheat biomass/waste including straw, bran, husk, and stalk as precursors for raw or untreated, chemically treated, carbonaceous, and composite adsorbents against various environmental pollutants. The influences of inlet pollutant amount, adsorbent dose, pH, temperature, and time on the performance of adsorbents against pollutants were considered. The maximum uptakes, equilibrium time, and adsorption nature were identified from isotherms, kinetic, and thermodynamic studies. The highest adsorbed amounts of most tested contaminants were 448.20, 322.58, and 578.13 mg/g for lead, chromium, and copper, 1374.6 and 1449.4 mg/g for methylene blue and malachite green, and 854.75, 179.21, and 107.77 mg/g for tetracycline, phosphate, and nitrate, respectively. For the studied adsorbate/adsorbent systems the adsorption mechanism and regeneration were also discussed. Significant results and future directions are finally presented.

Keywords: Crop wastes, adsorption, contamination, characterization, regeneration

46 **List of content:**

47 **1. Introduction**

48 **2. Wheat residues-based adsorbents**

49 **3. Adsorption of synthetic dyes**

50 **4. Adsorption of heavy metals**

51 **5. Adsorption of other contaminants**

52 **6. Regeneration and reusability of adsorbents**

53 **7. Conclusions and future prospects**

54

55

56

57

58

59

60

61

62

63

64

65

66

67

68

69

70

71

72 **1. Introduction**

73 Synthetic dyes, heavy metals, pesticides, pharmaceuticals, and other aquatic
74 contaminants represent an environmental and health threat owing to their hazardous nature (Xiao
75 et al., 2023). The primary source of these contaminants is the effluents from agro-industrial and
76 municipal activates (Mo et al., 2018; Solangi et al., 2021). Thus, such pollutants need to be
77 eliminated in order to protect water sources and to maintain water quality. For this purpose,
78 several methods have been suggested such as adsorption, membrane separation,
79 coagulation/flocculation, degradation, biological treatment, etc. (Rout et al., 2023). Among all
80 other techniques, adsorption is regarded as one of the most straightforward, adaptable, efficient,
81 insensitive to harmful substances, and commercially viable processes for treating wastewater
82 (Rashid et al., 2021).

83 Adsorption systems basically consist of adsorbents and adsorbates or pollutants. The
84 selection of suitable adsorbents with favorable performances against pollutants is a significant
85 step for efficient adsorption systems. Recently there is a focus on agricultural wastes as
86 precursors for adsorbents owing to their availability, renewability, eco-friendly nature, and
87 lignocellulosic composition (cellulose, hemicellulose, and lignin) (Othmani et al., 2022).
88 Moreover, the utilization of such wastes in the adsorption field has many advantages in terms of
89 producing cost-effective adsorbents relative to expensive commercial adsorbents like activated
90 carbon and also solving the problem of agricultural waste disposal (Tokula et al., 2023). Many
91 reviews have considered the utilization of agro-wastes such as bamboo (Kalderis et al., 2023),
92 rice husk (Shamsollahi & Partovinia, 2019), corn (Ahmed et al., 2023), eucalyptus
93 (Anastopoulos et al., 2022), peanut husk (Aryee et al., 2021), walnut shell (Albatrni et al., 2022),

94 rice straw (Foong et al., 2022), banana waste (Ahmad & Danish, 2018), and coconut residues
95 (Ighalo et al., 2023; Khan et al., 2023; James & Yadav, 2021) as precursors for adsorbents.

96 Wheat (*Triticum aestivum L.*) is the principal cereal crop that provides stable food for the
97 majority of the world's population. It is the second most widely grown grain after rice, thus it
98 releases more agro-waste materials. Globally, wheat is cultivated on an area of 214 million ha.
99 Wheat cultivation and processing generate large quantities of crop residue mainly include straw,
100 bran, and husk (Mohite et al., 2022). Such wastes have been utilized as animal feed (Yafetto et
101 al., 2023), fertilizer (Suresh et al., 2022), building materials (Jiang et al., 2023), source for
102 nanocellulose (Trivedi et al., 2023) and polysaccharides (Hou et al., 2015), and raw materials for
103 high value added products including bioethanol (Kumar & Prakash, 2023), sugar alcohol
104 (Bhavana et al., 2023), biogas (Rani et al., 2022), etc. Wheat wastes have also been suggested as
105 adsorbents against a variety of contaminants due to their preferred structure in terms of favorable
106 lignocellulosic composition and functionality.

107 There are very few review papers in the literature that discuss the use of wheat wastes-
108 based adsorbents to purify water. For example, the elimination of heavy metal ions using raw
109 wheat straw and wheat bran adsorbents (Farooq et al., 2010), and the use of wheat bran- based
110 materials as adsorbents for dyes (Chung et al., 2022). However, these reviews were specific in
111 terms of adsorbate or adsorbent and did not provide detailed information about the modification,
112 characterization, and regeneration of these adsorbents. Thus, this article is an extensive review of
113 recent data on the wheat residues-derived adsorbent/aquatic pollutant systems involving the raw
114 and modified (chemically treated, carbonaceous, and composite) adsorbent forms, characteristics
115 (pore properties, elemental composition, etc.), and adsorption performances. Isotherms, kinetics,
116 thermodynamics, and mechanisms of studied adsorption systems which are useful to identify the

117 maximum adsorption capacity, equilibrium time, adsorption nature, and main interaction steps,
118 respectively were also discussed. The common applied equations for isotherms, kinetics,
119 thermodynamics, and error functions are presented in Table S1 (supplementary data).
120 Regeneration ability and reuse of the exhausted adsorbents were also addressed.

121 **2. Wheat residues-based adsorbents**

122 Wheat (*Triticum aestivum L.*) belonging to the Poaceae family, is the second most
123 frequently grown cereal grain behind rice for human consumption (Chung et al., 2022). This crop
124 may be grown in Mediterranean, temperate, and subtropical climates due to its extensive genetic
125 diversity. Global worldwide production of wheat has been reported as 778.6 million metric tons
126 in 2021/2022 (Ammar et al., 2023). Large amounts of agricultural wastes are resulted from the
127 growing and processing of wheat which primary consists of straw, husk, and bran. These wastes
128 have many applications, for example wheat straw (stem, leaves, etc.) can be used as a soil
129 fertilizer, animal feed, and construction material, and feedstocks in fermentation industry, pulp
130 industry, and bioenergy generation such as bioethanol and biohydrogen (Khan & Mubeen, 2012).
131 Wheat bran is a byproduct of milling that possess both non-food and food qualities. It is an
132 excellent source of phenolic acids, dietary fiber, carotenoids, tocopherols, and enzyme synthesis
133 (Chung et al., 2022). Wheat husk flour was applied as filler in thermoplastic polymers like
134 polypropylene and high-density polyethylene in order to prepare their composites. Additionally,
135 it was employed in the production of thermal insulation panels, achieving a high thermal
136 insulation (Mohite et al., 2022).

137 In general, wheat wastes are lignocellulosic materials including cellulose, hemicellulose,
138 and lignin (Table 1), which consist of elements like C, H, N, and O. These materials possess
139 active groups like hydroxyl, amino, and carboxyl groups with high coordination capacity.

140 Therefore, these wastes in their raw or modified forms have been widely applied as adsorbents
141 for a variety of pollutant, as explained by the collected data of 115 papers (2010-2023) from
142 Google Scholar and Scopus database. The data showed that the most utilized wheat residues are
143 straw followed by bran, husk, and stalk, and the most applied wheat residues -based adsorbents
144 are in the form of chemically modified and biochar followed by raw, activated carbon,
145 composite, and hydrochar.

146 Raw or unmodified wheat residues were directly applied as adsorbents against aquatic
147 pollutants. In this regard, Chen et al. (2020a) investigated the composition and structure of wheat
148 straw and its application as adsorbent for Cr(VI) and Cr(III) ions. The chemical composition of
149 straw was 45.32% cellulose, 19.89% hemicellulose, and 12.49% lignin. The content of elements
150 was C 42.69%, O 49.96%, N 6.32%, and H 1.03%. Brunauer-Emmett-Teller (BET) surface area,
151 total pore volume, and average pore diameter were 12.576 m²/g, 0.030 cm³/g, and 3.045 nm,
152 respectively. The Fourier transform infrared (FTIR) spectrum of straw showed the existence of a
153 large number of surface active groups including –OH, N–H, C=O, C=C, C–O and C–H. Such
154 groups might play a significant role in the adsorption process of metal ions. Wheat bran biomass
155 with a specific surface area 5.7 m²/g was adopted as adsorbent for Cr(VI). The contents of acidic
156 and basic functional groups were 0.43 and 0.06 mmol/g, respectively (Ogata et al., 2020).
157 Moreover, wheat husk was used as adsorbent for congo red dye. The FTIR spectrum indicated
158 that different functional groups were appeared on the wheat husk surface including the hydroxyl
159 and amides groups (–OH and –NH) as well as C–O, C=O, C–H, etc. (Sabah & Alwared, 2019).

160 Chemically modified wheat wastes were adopted as adsorbents with enhanced
161 performance against a variety of pollutants. Several agents such as amines, alkalis, organic acids,
162 surfactants, iron oxides, etc. were applied for this purpose. The improvement in performance can

163 be attributed to the enhancement of functionality by introducing additional groups or enhancing
164 of the extent of original existing groups alone or with the development of porosity. Amino
165 modifications can increase the content of nitrogen and the extent of N–H group. In this regard,
166 wheat straw was modified by ethylenediamine/triethylamine and the nitrogen content was
167 increased significantly from 0.35% to 6.20%. This result suggested that large amounts of amine
168 groups grafted in treated straw. The performance against phosphate was 38.3 times that of raw
169 one (Xu et al., 2011a). Alkali, organic acids, and surfactants can enhance the extent of O–H, C–
170 O, and C–H groups, respectively. Accordingly, the performance of NaOH treated wheat straw
171 adsorbent against Cu(II) was 92.7% relative to 45.2% on raw straw (Guo et al., 2016). Moreover,
172 the performance of acetic acid modified wheat bran against Pb(II) was 87.72% relative to
173 56.32% on unmodified bran (Xing et al., 2013), and that of cationic surfactant, hexadecyl
174 trimethyl ammonium bromide (CTAB) modified wheat straw against congo red was 46.3 mg/g
175 relative to 23.0 mg/g on raw (Zhang et al., 2014a). On the other hand, magnetic modification can
176 introduce an additional Fe–O group and also can improve the surface area. It was found that the
177 surface area of raw and Fe₃O₄ treated wheat straws were 22.3 and 57.5 m²/g, respectively
178 (Pirbazari et al., 2014). Tian et al. (2011) showed that for Fe₃O₄ modified wheat straw, the
179 increase in iron concentration from 0.1 to 0.5M enhanced adsorption performance from 0.760 to
180 3.898 mg/g for As(III) and from 4.018 to 8.062 mg/g for As(V). Combining two or more
181 chemicals was also adopted for the modification purpose. For instance, Sodkouieh et al. (2023)
182 modified the wheat straw by NaOH/monochloroacetic acid. The alkali modification step could
183 dissolve the hemicellulose and lignin, and improved the straw reactivity against acid
184 modification. FTIR spectra of alkali/acid modified straw exhibited more intense carboxyl group
185 (Fig. 1) which favored the attraction of methylene blue cationic molecules.

186 Biochars were also prepared from wheat wastes and applied as adsorbents. According to
187 the collected data, wheat straw-derived biochar had a developed porous structure with the highest
188 BET surface area. In particular, it showed a large surface area of 343.56 m²/g, total pore volume
189 of 0.222 cm³/g, and average pore width of 2.549 nm at the pyrolysis conditions of 800 °C, 10
190 °C/min for 1 h under 50 mL/min N₂ flow (Wang et al., 2023a). In addition, a large specific
191 surface area of 260.9 m²/g was reported for biochar derived from wheat bran by pyrolysis at 800
192 °C for 2 h (Ogata et al., 2018). The literature also included other wheat residues such as husk
193 (Yuan et al., 2023) and stalk (Liu et al., 2022a) as precursors for biochars with maximum
194 reported BET surface areas of 46.5 and 158.98 m²/g, respectively.

195 Wheat wastes were also adopted as precursors for activated carbon (AC) using different
196 preparation methods. Activation by chemicals was the most widely applied method for the
197 preparation of AC from wheat wastes, as indicated from the collected data. Furthermore, several
198 chemicals like KOH, ZnCl₂, NaOH, H₃PO₄, etc. were used for the activation purpose. Among
199 these agents, ZnCl₂ was efficiently adopted for preparation of AC. In this regard, ZnCl₂
200 activation of pre-carbonized wheat straw at 3:1 alkali to pre-carbonized straw mass ratio, 800 °C
201 under N₂ flow for 2 h produced AC with the highest BET surface area of 2944 m²/g and total
202 pore volume of 1.33 cm³/g. The magnitude of 2944 m²/g was 5.7 times greater than that of wheat
203 straw biochar. This outcome was due to the etching role of ZnCl₂ towards biochar which resulted
204 in the formation of more micropores. The removal efficiencies of biochar and AC against
205 bisphenol A were 60.51% and 98.45%, respectively (Shi et al., 2022a). Moreover, KOH was
206 widely applied and exhibited a highest surface area of 1164 m²/g for wheat straw AC at the
207 activation conditions of 1:1 KOH to straw weight ratio, 800 °C, 1 h, and 10 °C/min (Alrowais et
208 al., 2023). The scanning electron microscope (SEM) image confirmed that KOH activation of

209 wheat straw biochar presented a well-developed porous structure (Fig. 2) with a large surface
210 area and more binding sites for Cr(VI) (Jamil et al., 2023). Other agents were adopted for
211 production of ACs from wheat residues. The reported surface areas were 2532 m²/g and 1123
212 m²/g for wheat bran/NaOH AC (Zhang et al., 2020a) and wheat straw/H₃PO₄ AC (Shou & Qiu,
213 2016), respectively. Physical activation of wheat straw with steam produced AC with a surface
214 area of 316 m²/g (Kwak et al., 2019).

215 The literature also involved wheat wastes-based composites and hydrochars as
216 adsorbents. For example, wheat bran-titanium dioxide (TiO₂) composite adsorbent for selenium
217 (Li et al., 2021), wheat straw biochar/biomass fly ash composite adsorbent for methylene blue
218 (Li et al., 2023), and montmorillonite-wheat straw biochar composite adsorbent for norfloxacin
219 (Zhang et al., 2018a). The performance of latter composite against norfloxacin was 2.29–2.60
220 times that of biochar alone, and montmorillonite alone had lower performance of 0.244–2.553
221 mg/g. Kohzadi et al. (2023) used Fe-modified hydrochar obtained from wheat straw as adsorbent
222 against the dye Rhodamine B with a best performance of 91%. Hydrochar was prepared at 200
223 °C for 6 h and modified with 0.1 M FeCl₃ solution. BET specific surface area, total pores
224 volume, and pore width were 52.74 m²/g, 0.3337 cm³/g, and 25.31 nm for Fe-modified
225 hydrochar relative to 9.40 m²/g, 0.0346 cm³/g, and 14.73 nm for pristine hydrochar, and 1.22
226 m²/g, 0.0021 cm³/g, and 6.86 nm for raw wheat straw. The FTIR spectrum of wheat straw,
227 original hydrochar and Fe-treated hydrochar showed O-H, C-O, C=C, and C-H groups. Fe-O
228 group was only being seen in Fe-modified hydrochar. Nzediegwu et al. (2021) applied wheat
229 straw-based hydrochar prepared at 180 °C, 240 °C and 300 °C for 4 h with 5 °C/min heating rate
230 as adsorbent for lead (II). Specific surface area was 4.1-4.5 m²/g; elemental composition was C

231 61.1-68.9%, H 4.6-4.0%, N 0.9-1.2%, and O 28.0-18.6%. The highest performance was reported
232 at 180 °C with 4.5 m²/g, 5.4% ash, pH 5.4, C 61.1%, H 4.6%, N 0.9%, and O 28.0%.

233 Thus, raw wheat residues with a favorable lignocellulosic content and excellent
234 functionality are widely applied as adsorbents. Moreover, the performance of these adsorbents
235 can be further improved by the development of their structure. The development involves the
236 enhancement of functionality alone or with the porosity. The developed wheat residues can be in
237 the form of chemically modified, biochar, activated carbon, hydrochar, and composite. From the
238 collected data, the largest surface areas for biochar and activated carbon derived from wheat
239 residues are reported as 343.56 and 2944 m²/g, respectively.

240 **3. Adsorption of synthetic dyes**

241 Dyes are coloured materials utilized in textile, cosmetic, pharmaceutical, rubber, plastic,
242 leather, printing, paper, and food industries to change or improve the colour of a substance
243 (Iwuozor et al., 2022). Their importance and usage in large amounts accounts for its existence in
244 the effluents of these industries. Specifically, these industries release about 700,000 tons (or
245 15%) of dyes annually into the aquatic environment, causing serious health and environmental
246 issues (Zhang et al., 2020b; Yaneva & Georgieva, 2013). In order to avoid such issues, many
247 researchers have suggested the use of different materials like wheat residues-based adsorbents
248 for the removal of dye molecules from the aquatic systems. Table 2 shows that most studies
249 focused on the elimination of cationic methylene blue dye followed by malachite green, methyl
250 orange, congo red, crystal violet, etc.

251 The removal of methylene blue (MB) was tested using wheat straw (Ben'ko & Lunin,
252 2018), wheat husk modified with perchloric acid (Banerjee et al., 2014), phytic acid-treated

253 wheat straw (You et al., 2016), Fe₃O₄-wheat straw (Pirbazari et al., 2014), and citric acid
254 modified wheat straw (Han et al., 2010). The pH factor had an effect on the MB adsorption
255 process depending on the type of adsorbent. For instance, the removal percentage increased from
256 40.7% to 96.2% by changing the pH of the solution from 4.5 to 9.5, using wheat husk treated
257 with perchloric acid (Banerjee et al., 2014). In another work (You et al., 2016), the MB uptake
258 by phytic acid-modified wheat straw was found to increase by raising the pH from 2.0 to 10,
259 giving approximately a maximum uptake of 205.4 mg/g. Another team (Pirbazari et al., 2014)
260 also found that an increase in pH, affected positively the removal of MB by Fe₃O₄-wheat straw,
261 and maximum uptake was reported at pH 7.0 (pH studied range of 2.0–12.0). Contact time is
262 another factor that impacts the adsorption process. Banerjee et al. (2014) and You et al. (2016)
263 concluded that 50 min are sufficient to attain equilibrium for the removal of MB by perchloric
264 acid modified wheat husk and phytic acid modified wheat straw, respectively. The adsorbent
265 dose also affects the ability to remove the MB dye. The removal efficiency of MB enhanced
266 from 79.80 to 93.4% and from 36% to 96% by changing the dose from 10 to 25 g/L and 0.1 to 1
267 g/L, using wheat husk modified with perchloric acid (Banerjee et al., 2014) and Fe₃O₄-wheat
268 straw (Pirbazari et al., 2014), respectively. Another crucial adsorption parameter is the solution
269 temperature. The rise of temperature from 303 to 323 K was found to reduce the adsorption
270 efficiency from 93.4% to 59.8% using perchloric acid treated wheat husk (Banerjee et al., 2014).
271 On the contrary, Han et al. (2010) explored the utilization of citric acid-modified wheat straw
272 and noticed that with the increment of 293 K to 313 K the maximum monolayer adsorption
273 obtained from Langmuir isotherm increased from 396.9 to 450.0 mg/g. Another study concluded
274 that the temperature change from 298 – 323 K, had little effect on the MB uptake (the maximum
275 uptake q_{\max} from Langmuir isotherm decreased from 217.4 mg/g to 215.9 mg/g) by phytic acid-

276 modified wheat straw (You et al., 2016). Thermodynamic studies showed that the adsorption of
277 MB onto different adsorbents was mostly spontaneous (Banerjee et al., 2014; Han et al., 2010),
278 exothermic (Banerjee et al., 2014) or endothermic (Han et al., 2010) with increasing (Han et al.,
279 2010) or even decreasing (Banerjee et al., 2014) randomness at the solution/solid interface.
280 Sodkouieh et al. (2023) showed that the adsorption mechanism of MB on carboxymethylated
281 wheat straw involved different types of interactions (Fig. 3) including electrostatic attractions,
282 Yoshida H-bonding, dipole-dipole H-bonding, and $n-\pi$ interaction.

283 Wheat straw-based adsorbents were also used to remove other cationic dyes such as
284 Rhodamine B (RhB), malachite green (MG), and crystal violet (CV). For example, Kohzadi et al.
285 (2023) explored the application of raw and Fe-treated hydrochars and biochars obtained from
286 wheat straw to adsorb RhB. FeCl₃ wheat straw hydrochar appeared to have more voids, porosity,
287 and roughness. The maximum uptake of RhB by Fe-treated hydrochar was 80 mg/g at 1 g/L of
288 adsorbent dosage, 1.5 h of contact time, inlet dye amount 2.5–25 mg/L, pH 6.0, agitation speed
289 of 120 rpm, at room temperature (25 °C). Mean free energy (E) from Dubinin-Radushkevich (D-
290 R) model was 7.07 kJ/mol indicated that physisorption played an important role in the removal
291 of RhB by Fe-modified hydrochars. Another team (Yang et al., 2019) utilized wheat straw and
292 wheat bran as precursors for the production of biochars at various pyrolysis temperatures (400,
293 600, and 800 °C). The aforementioned wheat straw (WSBC) and wheat bran (WBBC) derived
294 biochars were applied for MG and CV dyes removal. The highest uptakes of these dyes were
295 obtained from biochars fabricated at 800 °C and WSBC-800 gave the highest adsorption capacity
296 against MG. The maximum uptake of MG was estimated to be 1449.4 mg/g and 1301.9 mg/g, for
297 WSBC-800 and WBBC-800, respectively. Another team (Haq et al., 2021) explored the
298 utilization of wheat bran to adsorb the CV dye. Maximum adsorption of 92.51% and 89.73% was

309 noticed at pH 2.0 (pH studied range from 1.0 – 11) and at 120 min of contact time (contact time
300 studied range from 5–120 min), respectively. Thermodynamic results (temperature range 273 K
301 to 333 K) showed that the CV adsorption onto wheat bran was spontaneous and endothermic
302 with enhancing randomness at the solution/solid interface. The increment of temperature from
303 273 K to 333 K caused an increase in adsorption percentage of CV dye from 85.5% to 86.5%.

304 The adsorption behavior of wheat straw and various derivatives has also been
305 investigated on aqueous solutions of anionic dyes. Specifically, three works modified wheat
306 straw with surfactants (Zhang et al. 2014a, 2017, 2018b), two groups enriched wheat straw with
307 inorganic acids or salts (Mirjallili et al. 2011, Mohammadi et al. 2021), whereas one group
308 prepared a magnesium hydroxide-coated biochar (Zhang et al. 2014b).

309 Based on the summary of Table 2, in most cases adsorption best matched the pseudo-
310 second order kinetic model and the Langmuir isotherm model. Furthermore, all studies agreed to
311 an optimum pH range between 3-4, revealing that the process was largely limited by electrostatic
312 interactions between the anionic dye and cationic moieties on the adsorbent surface. In most
313 cases, adsorption was spontaneous and exothermic, which is attributed to the tendency to reduce
314 the internal energy to attain a thermodynamically stability (Chanajaree et al., 2021). However,
315 the adsorption of direct yellow 12 on wheat straw biochar and acid red 18/acid black 1 on
316 surfactant modified wheat straw, showed an endothermic behavior. Since the ΔH° values for
317 these cases were below 40 kJ/mol, chemisorption is unlikely (Akpomie & Conradie, 2023). A
318 possible explanation may be that the molecules of these dyes require the additional energy to
319 move faster and penetrate deeper into the pores of the adsorbent (Al-Ghouti & Al-Absi, 2023).

320 **4. Adsorption of heavy metals**

321 Heavy metals are widely recognized as the most common and toxic inorganic
322 contaminants in water and soil systems (Haris et al., 2021; Saleem et al., 2023). The rapid
323 growth of the global economy, population, and industrialization has resulted in a significant
324 increase in severe metal pollution and associated threats to the environment and human health
325 (Filippini et al., 2022). Therefore, the removal of heavy metals from contaminated water matrices
326 has become a matter of great concern. From the gathered data (Table 3), the most studied metals
327 are lead followed by chromium, copper, cadmium, nickel, zinc, mercury, etc.

328 Wheat residues-based adsorbents, particularly after appropriate modification, are showing
329 great potential in removing heavy metals from the water environment. Their efficiency is,
330 however, affected by various factors, including their physicochemical properties, solution pH,
331 adsorbent dosage, and contact time (Dong et al., 2019; Lu et al., 2020). The modification of
332 wheat-residue-derived adsorbents further enhances their efficiency compared to their pristine
333 forms. Various methods have been explored for this, such as modifying raw wheat straw itself,
334 transforming it into other carbonaceous adsorbents like biochar, or further modifying the
335 converted forms to enhance their effectiveness. Several methods have been employed to modify
336 wheat straws for enhanced efficiency in adsorption. These include the use of citric acid (Han et
337 al., 2010), diethylenetriamine and N,N-dimethylformamide (Chen et al., 2010), magnetization
338 (Tian et al., 2011), amine (Xu et al., 2011a), tartaric acid (Kaya et al., 2014), calcination (Ogata
339 et al., 2018), polyethylenimine (Dong et al., 2019), carbonization and ball milling (Cao et al.,
340 2019a), and compositing with TiO₂ (Li et al., 2021).

341 In addition to directly enhancing the properties of wheat-straw, the conversion of wheat
342 straw into biochar has been recognized as a promising strategy to develop carbonaceous
343 adsorbents with high metal removal efficiency (Wang et al., 2010; Wang et al., 2011; Cao et al.,

2019b; Zhang et al., 2022; Shen et al., 2017). Moreover, the modification of these biochars has further improved their treatment efficiency against toxic metals. Examples of such modifications include nano-chlorapatite modification of wheat-straw-based biochar (Yuan et al., 2023) and the exfoliation process to produce exfoliated biochar (Haris et al., 2022). For instance, Haris et al. (2022) compared the efficiency of pristine wheat-straw derived biochar (PB) and its HNO₃ treated or exfoliated biochar forms (EBFs) towards thallium Tl(I) adsorption in an aquatic environment. They found that EBFs exhibited a significantly higher specific surface area (421.24 m²/g) and pore size (3.98 nm) compared to PB (3.81 m²/g and 2.05 nm, respectively). When used for Tl(I) adsorption, EBFs showed superior adsorption capacity (382.38 mg/g) at pH 7.0, which was over 9 times greater than that of PB.

Adsorption isotherm models are widely applied to evaluate adsorbent- adsorbate interactions at equilibrium adsorption (Hamid et al., 2022). The isotherm study describes the distribution of metal ions between liquid and solid phases, providing valuable insights into the adsorption process (Sinha et al., 2022; Ambika et al., 2022). Several adsorption models including Freundlich, Langmuir, Temkin, Redlich-Peterson, Dubinin-Radushkevish, etc. have been applied to evaluate the adsorption behaviour of heavy metals (Muhammad et al., 2021; Chen et al., 2022). The Langmuir and Freundlich isotherm models are frequently used to examine the adsorption of heavy metals. The Langmuir isotherm has been particularly suitable to describe the heavy metals adsorption onto wheat residues-based adsorbents as it represents the monolayer adsorption behaviour, characterized by a homogeneous distribution of adsorbate molecules without significant interactions among them (Zhang et al., 2022; Li et al., 2021). The Freundlich isotherm, however, describes the multilayer adsorption behavior and has proven to be a good fit for heavy metals adsorption in certain cases, involving heterogeneous chemisorption processes.

367 For instance, Chen et al. (2010) observed Cr(VI) adsorption on modified wheat-straw at different
368 temperature (298, 313, and 328 K). They found that Freundlich adsorption model had a higher
369 determination coefficient R^2 (0.941, 0.958, and 0.991) than Temkin (0.903, 0.925, and 0.971) and
370 Langmuir model (0.759, 0.770, and 0.857). This indicates that modified wheat-straw exhibit
371 multilayer adsorption behavior on heterogeneous surfaces, characterized by a finite number of
372 sites with interactive properties.

373 Similarly, the evaluation of adsorption kinetics provides valuable perceptions into the
374 underlying mass transfer adsorption process, including any rate-controlling step involved
375 (Plazinski et al., 2009). Various kinetics equations like pseudo-first-order PFO, pseudo-second-
376 order PSO, Elovich, and intra-particle diffusion IPD were used to determine the adsorption
377 capacity of heavy metals dictated by the reaction time (Han et al., 2010). In most of the studies
378 on the removal of heavy metals using wheat residues-based adsorbents, the PSO model exhibited
379 the best fit (Table 3). This has been attributed to the rate-limiting step associated with this model,
380 whereby the availability of binding sites on the biochar surface is influenced by chemical
381 reaction rates (Tian et al., 2011; Bandara et al., 2020). PSO model effectively describes the solid-
382 liquid reaction and elucidates the kinetics mechanism of adsorption, emphasizing that the
383 adsorption process is primarily governed by the availability of binding sites rather than the
384 amount of heavy metals (Farooq et al., 2011). For instance, Fu et al. (2021) applied various
385 kinetics equations (PFO, PSO, and Elovich) to approximate the adsorption kinetics of Cd(II)
386 onto magnetic biochar derived from wheat straw. They extrapolated that PSO model provides the
387 best analysis with the largest R^2 (0.99) than PFO model (0.98) and Elvoich model (0.92),
388 confirming chemisorption as the rate-limiting step for Cd(II) adsorption.

389 Thermodynamic studies are intended to evaluate the impact of temperature on
390 contaminant adsorption. Thermodynamic constants, involving free energy (ΔG°), entropy (ΔS°)
391 and enthalpy (ΔH°); provide insights into the endothermic or exothermic nature of the adsorption
392 process (Chen et al., 2020a). The adsorption process is favoured at high temperatures as, for
393 instance, observed in the adsorption of heavy metals onto wheat residues-based adsorbents that
394 was found to be thermodynamically spontaneous (Ogata et al., 2018). A negative ΔH° value
395 suggests an exothermic nature of adsorption, whereas a positive ΔH° value indicates an
396 endothermic process. Furthermore, a positive ΔS° value affirms enhanced randomness associated
397 with the adsorption of heavy metal ions (Ogata et al., 2013; Wang et al., 2019). Numerous
398 experimental findings have consistently demonstrated the endothermic nature of heavy metal
399 removal, as indicated by the positive values of ΔH° . For example, Zhu et al. (2016) applied
400 bismuth-modified biochar prepared from wheat-straw for the adsorption of As(III) and evaluated
401 the thermodynamic parameters. Their findings revealed a positive ΔH° value ($11.86 \text{ kJ mol}^{-1}$),
402 demonstrating the favourable endothermic nature of As(III) adsorption onto the biochar. The
403 positive ΔS° value (0.15 kJ/mol) suggested an increase in the disorder of the solid-solution
404 interface and the negative ΔG° value (-32.48 kJ/mol) suggests the co-existence of chemisorption
405 and physisorption during the adsorption process.

406 The metal adsorption efficacy of wheat residues-based adsorbents predominantly relies
407 on factors such as its specific surface area, cation exchange capacity and abundance of surface-
408 active functional groups (Cao et al., 2019b). For example, the existence of surface functionalities
409 such as phenolic, carboxylic and hydroxyl ($-\text{COO}^-$ and $-\text{OH}^-$) enhanced the number of
410 negatively-charged active sites on wheat residues-based adsorbents. These sites were found to
411 effectively bind with cationic metals including Cu(II), Tl(I), Zn(II), Pb(II) and Cd(II) in water

412 matrices (Zama et al., 2017). In addition, the existence of electron donor active groups (C–O–R,
413 –C–OH, C–O) facilitated the adsorption of Cr(VI) on biochar obtained from wheat-straw, with
414 adsorption-coupled reduction of Cr(VI) into Cr(III) to enable surface adsorption (Wang et al.,
415 2010; Xu et al., 2011a). These findings suggest that the characteristics of wheat residues-based
416 adsorbents, such as ionic content, organic functional groups, π -electrons and mineral content,
417 have a direct impact on adsorption mechanisms of heavy metals and determine the adsorption
418 capacity of wheat residues-derived materials for heavy metals in contaminated water
419 environment. Adsorption is a universal term to describe all the processes at the wheat residues-
420 based adsorbents–solution interface, involving chemisorption, surface complexation,
421 intermolecular attractions, precipitation/co-precipitation, ion exchange and magnetic bonding
422 (Yuan et al., 2023). The adsorption process of heavy metals onto wheat residues-based
423 adsorbents is not governed by a single mechanism, but rather involves a combination of multiple
424 mechanisms. For instance, Nzediegwu et al. (2021) showed that the adsorption mechanism of
425 Pb(II) on wheat straw derived biochar/hydrochar was represented by electrostatic attraction,
426 cation exchange, complexation, and precipitation (Fig. 4). Another team Cao et al. (2019a)
427 studied the Pb(II) adsorption mechanism by pristine wheat-straw, wheat-straw biochar and ball-
428 mill modified wheat-straw biochar. They reported that precipitation (i.e., PbCO_3 and
429 $\text{Pb}_3(\text{CO}_3)_2(\text{OH})_2$), complexation (-COOH and -OH) and ion-exchange (Ca(II), Mg(II), K(I), and
430 Na(I)) were the dominant mechanisms involved in adsorption process.

431

432 **5. Adsorption of other contaminants**

433 Pharmaceuticals, inorganic anions and cations, phenols, herbicides, etc. are also
434 eliminated from aqueous solutions by using wheat wastes-based adsorbents. Tetracycline, nitrate,

435 phosphate, ammonium, and 2,4-dichlorophenoxyacetic acid (2,4-D) herbicide are examples of
436 aquatic pollutants that widely tested in the literature relative to other pollutants (Table 4).

437 Wang et al. (2021) used diethylenetriamine, chloroacetic acid, and zirconium modified
438 wheat straw (Zr-WS) adsorbent for the removal of tetracycline (TC). The adsorbent exhibited
439 remarkable adsorption ability along with some selectivity against tetracycline due to the
440 zirconium oxychloride and hydroxyl-enriched structure of Zr-WS. The adsorbed amount of TC
441 onto Zr-WS was 77.2 mg/g at 303 K. Freundlich equation showed suitable fit to the isotherm
442 data with R^2 (0.984-0.992) and square of error SSE (14.8-17.7) relative to R^2 (0.963-0.993) and
443 SSE (7.33-65.4) for Temkin, while Elovich equation was better to analyze the kinetic data with
444 R^2 (0.971-0.996) and SSE (0.596-56.4) $\times 10^{-2}$ relative to R^2 (0.927-0.986) and SSE (0.508-
445 2.710) $\times 10^{-2}$ for PSO. Equilibrium and kinetic results confirmed that the TC/Zr-WS system had a
446 heterogeneous, multi-layer, and chemisorption nature. The thermodynamic parameters in terms
447 of $\Delta H^\circ > 0$, $\Delta G^\circ < 0$, and $\Delta S^\circ > 0$ affirmed that the studied adsorption system was endothermic
448 and spontaneous with increased entropy. ΔH° (kJ/mol) 56.3, ΔS° (J/mol.K) 211, and ΔG°
449 (kJ/mol) -5.46, -8.51, and -9.70 at 293K, 303K, and 313K, respectively. The mechanism of TC
450 adsorption on Zr-WS might involve coordination complexation, electrostatic attraction, and ion
451 exchange. Increasing pH from 2 to 7 enhanced TC uptake from 35.0 to 57.5 mg/g, respectively
452 for the sample of 100 mg/L. Huang et al. (2023) also tested the adsorption of tetracycline on
453 KMnO_4 activated wheat straw biochar (Mn-BC). The KMnO_4 modification increased the
454 adsorption performance against TC by developing the pore and surface characteristics of the
455 biochar. Mn-BC exhibited the largest uptake of 107.77 mg/g for TC, which was 3.4 times more
456 than that of original biochar (32.12 mg/g). The best removal by raw and activated biochars was
457 reported at pH 7 and 5, respectively. The Freundlich and PSO equations well analyzed the data

458 of TC/Mn-BC system. The mechanism (Fig. 5) of studied system involved the electrostatic
459 interaction, hydrogen binding, pore filling, and π - π interaction.

460 Chemically modified wheat residue in terms of H₂SO₄ modified wheat husks (*Fagopyrum*
461 *Esculentum*) was efficiently applied for adsorption of 2,4-D herbicide (Franco et al., 2021).
462 Regarding the optimum conditions, the best removal was reported at the pH 2 and the dosage of
463 0.95 g/L showed the best correlation between the removal efficiency and uptake of herbicide.
464 The kinetic data were well represented (R^2 0.9915-0.9985) by the Avrami fractional- order
465 equation (also known as Bangham), and the adsorption achieved equilibrium at lower than 150
466 min. The maximum uptake was 161.1 mg/g at 298K according to the Liu equation (R^2 0.9992-
467 1.000). From the thermodynamic parameters, the studied system was exothermic, spontaneous,
468 and preferable, and the adsorption mechanism involved electrostatic interactions, H-bonding, and
469 π - π interaction. More favorable adsorption was obtained under the acidic media as compared to
470 the alkaline media. This result could be attributed to the higher affinity of 2,4-D for the water
471 and strong repulsion between the anionic 2,4-D (pK_a=2.81) and negatively charged adsorbent
472 surface (pH_{PZC}=3.5) at higher pH. The uptake was increased from 25 to 80 mg/g with the change
473 of inlet 2,4-D amount from 50 to 200 mg/L due to the enhanced driving force for mass transfer.

474 Another team (Wang et al., 2016) studied the adsorption of atrazine on wheat straw-
475 biochar obtained at 750 °C (WS750). The Langmuir model (R^2 0.996) was more accurate to
476 represent the sorption isotherm of atrazine than Freundlich equation (R^2 0.982). PSO model (R^2
477 0.995) could present a well-analysis for the sorption kinetic of atrazine than PFO (R^2 0.901).
478 Thus, the studied system had the monolayer and chemisorption nature. The value of q_{\max} was
479 20.161 mg/g and the equilibrium nearly arrived after 80 h. The uptake of atrazine by WS750 was
480 favorably proportional to the inlet atrazine amount. The sorption quantities of atrazine by WS750

481 gradually decrease (33.50 to 22.71 mg/g) with the increased pH values (from 5 to 9). WS750
482 exhibited high affinity for atrazine in low pH medium as compared to high pH medium due the
483 favorable interaction with aromatic ring and positively charged (protonated) N atoms of atrazine.

484 Raw and ZnCl_2 activated wheat straw biochars were used as adsorbents against 4-
485 chlorophenol 4-CP (Shen et al., 2021). Adsorption ability of activated biochar was nearly 4 times
486 more than that of raw biochar which could be due the significant development in the oxygenated
487 active groups and surface area; in particular, the surface area of activated biochar was about 126
488 times that of raw. For ZnCl_2 modified (activated) wheat straw biochar, Langmuir exhibited R^2
489 (0.9771-0.9893) compared to R^2 (0.9740-0.9862) for Freundlich model. The high R^2 values of
490 these two models suggested the existence of both heterogeneous and homogeneous adsorption.
491 The values of q_{\max} were 111.02, 105.07, and 94.15 mg/g at 20 °C, 30 °C, 40 °C, indicating an
492 exothermic adsorption. Adsorption of 4-CP on activated biochar attained equilibrium state in 720
493 min. PSO showed high R^2 (0.9809-0.9965) relative to R^2 (0.9228-0.9608) for PFO, indicating the
494 chemisorption. The rate-limiting step was not represented by the intraparticle diffusion alone, as
495 proved by Weber-Morris equation. Due to ΔG° -21.86, -21.26, -21.18 kJ/mol (293, 303, 313K)
496 and ΔH° -31.99 kJ/mol < 0, the adsorption system was exothermic and spontaneous. ΔS° -34.82
497 J/mol.K < 0 suggested a decreased entropy process. Activated biochar showed a best removal (~
498 87%) of 4-CP within the pH from 4 to 8. This could be due to the promoted electrostatic forces
499 between the protonated phenolic -OH group of 4-CP ($\text{pK}_a = 9.3$) and the negatively charged
500 surface of biochar ($\text{pH}_{\text{PZC}} = 2.57$). The hydrogen bonding, van der Waals forces, electrostatic
501 interaction and π - π interaction could represent the mechanism of tested system.

502 Shou & Qiu (2016) studied the kinetics of phenol adsorption onto wheat straw/ H_3PO_4
503 AC. PSO kinetic model exhibited high R^2 0.9974 relative to R^2 of 0.8998 and 0.8381 for PFO

504 and Elovich models, respectively for the sample of 500 mg/L initial phenol concentration. The
505 PSO kinetic equation implied that the process was predominated by chemisorption which
506 involved valency forces through electrons sharing between adsorbent and adsorbate. The
507 equilibrium was attained at 40 min with an uptake of 270.61 mg/g for the sample of 500 mg/L
508 initial phenol concentration. The plot of the intraparticle diffusion equation revealed that the rate-
509 limiting step was identified by the pore diffusion along with other mechanism like boundary
510 layer.

511 Shahaji et al. (2023) examined the performance of raw wheat straw for the elimination of
512 nitrate from aqueous solution. The adsorption performance of straw against the NO_3^- was within
513 the range from 22 % to 53 %. The best result was reported at contact time = 3 h, straw amount =
514 3 g, and inlet nitrate amount = 700 mg/L. Langmuir equation well applied to describe the
515 adsorption isotherm (R^2 0.71), suggesting a monolayer adsorption on homogeneous adsorbent
516 sites. From the Langmuir equation, the value of q_{\max} was 94.25 mg/g and the value of separation
517 factor (R_L 0.4859) was between 0 and 1 which confirmed favorable adsorption. The enhancement
518 in straw dosage and inlet nitrate amount improved the nitrate adsorption due the availability of
519 more binding sites and the existence of more NO_3^- ions, respectively.

520 Bifunctional adsorbent in terms of La-Ca-quaternary amine-modified straw was adopted
521 for adsorption of phosphate and nitrate from nutrient-polluted water (Zhang et al., 2023). The
522 mechanism of adsorption included electrostatic attraction, ion exchange, inner-layer
523 complexation, and surface precipitation. Both the Langmuir and Freundlich equations well fitted
524 the isotherm data of nitrate with $R^2 > 0.94$, which implied the existence of mono- and multi-layer
525 adsorption. Meanwhile, the Langmuir model (R^2 0.960) better correlated the data of phosphate as
526 compared to the Freundlich equation (R^2 0.883), suggesting monolayer adsorption. The

527 experimental data of nitrate were well fitted to PSO and PFO kinetic models with $R^2 > 0.92$,
528 indicating the existence of chemical and physical adsorption. The PSO kinetic equation
529 ($R^2=0.954$) well fitted the adsorption data of phosphate, confirming the chemisorption.
530 Phosphate took 8 h to reach adsorption equilibrium, but nitrate reached it in just 3 h. Nitrates
531 exhibited a strong affinity for the quaternary amine active groups provided by amine
532 modification, while phosphates adsorbed on the metal-active groups more slowly. The uptake of
533 nitrate was shown to be rather steady across the pH from 3 to 10, and declined considerably at
534 pH values below 3 and above 10. In a lower pH solution, more H^+ ions were existed which
535 hindered the attraction of NO_3^- ions towards the quaternary amine active groups. However, the
536 more negatively charged adsorbent surface in a higher pH solution (the pH of adsorbent at the
537 zero-point charge (pH_{PZC}) = 10.81) caused nitrate to be repelled electrostatically. Furthermore, a
538 large quantity of OH^- competed with NO_3^- for the quaternary amine active sites, which reduced
539 the adsorption performance. Moreover, La-Ca-MWS demonstrated a high phosphate uptake
540 (49.5–92.2 mg/g) within a wide range of pH from 2 to 12.

541 **6. Regeneration and reusability of adsorbents**

542 Reusability studies by carrying out multiple adsorption/desorption cycles are necessary to
543 minimize the cost of the fabrication of adsorbents. An ideal spent/exhausted/used adsorbent must
544 have both high desorption and adsorption capability for commercial and industrial applications
545 (Baskar et al., 2022). Alkalis, acids, alcohols, salts, etc. have been applied for regenerating wheat
546 wastes-based adsorbents loaded with various contaminants, as summarized in Table 5.

547 Among these, NaOH and HCl were widely applied as eluents. NaOH was better than
548 several agents in regenerating of exhausted wheat residues-derived adsorbents. For example, Shi
549 et al. (2022b) investigated the regeneration ability of amine-modified wheat straw loaded with

550 nitrate by using different kinds of reagents such as NaOH, HCl, and NaCl. Results showed that
551 0.1M NaOH exhibited a better regeneration performance (93.6%) than 0.1M HCl (87.2%) and
552 0.1M NaCl (69.1%). The larger regeneration performance of NaOH relative to other agents was
553 also reported for KMnO_4/KOH modified wheat straw biochar loaded with tetracycline (Xu et al.,
554 2022), KMnO_4 activated wheat straw biochar loaded with tetracycline (Huang et al., 2023),
555 perchloric acid modified wheat husk loaded with acid orange 10 (Banerjee et al., 2016).
556 Moreover, exhausted wheat based adsorbents regenerated with NaOH exhibited a slight decrease
557 in their performance within high regeneration cycles. In this context, a slight decrease in removal
558 percentage of 2,4-D herbicide (2.18%) was reported for the H_2SO_4 modified wheat husks
559 regenerated by 0.5M NaOH within 5 cycles (Franco et al., 2021). Also, Ogata et al. (2020)
560 showed that the calcined wheat bran loaded with Cr(VI) could be regenerated by 1M NaOH with
561 only 1% decrease in regeneration performance within 5 cycles. Tian et al. (2011) used 0.1 M
562 NaOH for the desorption of arsenic from magnetic (Fe_3O_4) wheat straw at 30 °C for 3 h. After 10
563 recycling times, the removal efficiency of arsenic was still higher than 80%. Thus, this material
564 would be useful in practical industrial applications.

565 HCl was applied for desorption of pollutants from exhausted wheat-based adsorbents.
566 Nzediegwu et al. (2021) showed that 0.1M HCl eluent exhibited high regeneration performances
567 of 92% and 100% for Pb(II) loaded wheat straw biochar and hydrochar, respectively. The
568 findings showed that Pb(II) would be stable on the adsorbents in an almost neutral medium but
569 would become much less stable in an acidic medium. Moreover, 0.1M HCl could efficiently
570 regenerate Pb(II) loaded adsorbents, as opposed to deionized water. Another team (Shi et al.,
571 2022b) reported that 0.1M HCl could exhibit a regeneration performance of 87.2% for amine
572 modified wheat straw loaded with nitrate. Qi et al. (2023) showed that the largest desorption

573 efficiencies of wheat straw biochar were 96.07%, 76.17%, and 56.22% for Cd^{2+} , Cu^{2+} , and Pb^{2+} ,
574 respectively using 2M HCl. Sodkouieh et al. (2023) showed that 0.01M HCl was better than
575 0.01M NaCl and distilled water for the regeneration of methylene blue loaded
576 NaOH/monochloro acetic acid modified wheat straw. The reported regeneration performance of
577 0.01M HCl was 84.8%. Zhang et al. (2020a) showed that 0.2M HCl was able to regenerate Pb(II)
578 loaded wheat bran/NaOH AC with high adsorption performance of about 99% at the first
579 regeneration cycle and only 4% decrease in adsorption performance within 4 cycles. HNO_3 was
580 also used as a regenerating agent. Wheat straws loaded with the Cr(III) ions were regenerated
581 with 0.1 M HNO_3 solution (Chen et al., 2020a). There was no significant change (46.875-44.0
582 mg/g within 10 cycles) in the uptake of metal ions during the frequently recycling experiments,
583 suggesting the effective reusability of adsorbent. Zhang et al. (2018c) showed that the
584 regeneration performance was in the order $\text{HNO}_3 > \text{NaNO}_3 > \text{H}_2\text{O}$ for wheat straw biochar
585 loaded with Hg(II).

586 Alcohols like methanol and ethanol were also applied as eluents for the regeneration
587 purpose. Zhang et al. (2018a) used methanol for the regeneration of montmorillonite-wheat straw
588 derived biochar composite loaded with norfloxacin. The regeneration performance was 86.8% at
589 the first cycle and a slight decrease of 0.3% was reported in the regeneration performance within
590 5 cycles. H-bond between methanol and norfloxacin was stronger, which resulted in an easy
591 elimination of norfloxacin. Wang et al. (2016) also tested the regeneration of wheat straw- based
592 biochar loaded with atrazine using methanol. The uptake of atrazine by biochar was reduced
593 from 31.2 mg/g to 22.3 mg/g within 3 regeneration cycles. Thus, 72% of adsorbent performance
594 was retained after 3 times regeneration with methanol. Shi et al. (2022a) showed that ethanol and
595 methanol were effective with high performances of 92.86% and 83.31% in regenerating ZnCl_2

596 activated wheat straw-derived biochar loaded with bisphenol A. For regeneration by ethanol, the
597 adsorbent performance was 98.3 mg/g at the first cycle and dropped to 82.8 mg/g at the fifth
598 cycle. The highest regeneration efficiency of ethanol was due to its ability to weaken the π - π
599 interaction and hydrogen bonding between the adsorbate and adsorbent. Zhang et al. (2018b)
600 reported that the use of ethanol (75 vol%) showed a maximum regeneration performance of
601 78.68% for the CTAB surfactant- modified wheat bran loaded with acid red 18 dye.

602 Other eluents were also included in the literature. Mehdinejadani et al. (2019) used NaCl
603 saturated solution for the desorption of nitrate from silane/octane treated wheat straw. NaCl was
604 able to recover about 97.3% of the loaded nitrate and the removal percentage of nitrate was
605 slightly decreased by about 2.4% within five regeneration cycles. This could be attributed to the
606 insignificant weight loss of adsorbent during the regeneration process. Chen et al. (2020a)
607 regenerated the Cr(VI)-loaded wheat straws with 1 M KOH Solution. Within 10 cycles, the q
608 values for Cr(VI) decreased from 80.625 to 76.875 mg/g during the regeneration of Cr(VI)
609 loaded wheat straw by 1M KOH. Thus, there was no significant change (3.75 mg/g) in the
610 adsorption capacities during the frequent regeneration, confirming the effective reusability of the
611 straws. Zhang et al. (2023) showed that the adsorption performance of La-Ca-quaternary amine
612 (trimethylamine)-treated wheat straw against nitrate and phosphate was greater than 85% (~87
613 %) after nine regeneration cycles with a 10 % NaOH–NaCl mixture. This adsorbent could be
614 practically applied in the elimination of inorganic anions from water.

615 From the above discussion, it can deduce that wheat residues-based adsorbents can be
616 efficiently regenerated by different agents, and frequently utilize for removal of various aquatic
617 contaminants. The most widely adopted eluents for regeneration purpose are NaOH and HCl.
618 Thus, these adsorbents will be useful for practical and economic applications.

619 7. Conclusions and future prospects

620 Wheat residues-based adsorbents in their raw and modified forms against various aquatic
621 contaminants have been reviewed. The most used residues were straws followed by brans, husks,
622 and stalks. Moreover, the most applied wheat residues-based adsorbents were in the forms of
623 chemically modified and biochar followed by raw, activated carbon, composite, and hydrochar.
624 In general, the modified adsorbent forms exhibited enhanced performances relative to
625 unmodified or pristine form. The enhancement could be attributed to the development in
626 functionality with or without improvement in pore properties. Most of the collected data were
627 related to methylene blue and malachite green dyes, lead, chromium, and copper metal ions, and
628 tetracycline antibiotic along with inorganic anions in terms of phosphate and nitrate. The
629 maximum adsorbed amounts of these contaminants were 448.20, 322.58, and 578.13 mg/g for
630 lead, chromium, and copper, 1374.6 and 1449.4 mg/g for methylene blue and malachite green,
631 and 854.75, 179.21, and 107.77 mg/g for tetracycline, phosphate, and nitrate, respectively. The
632 adsorbents performance mainly dependent on inlet pollutant amount, adsorbent dose, solution
633 pH, temperature, and contact time. PSO kinetic and Langmuir/Freundlich isotherm equations
634 well fitted the adsorption data in most of the studies. Temkin, Sips, Redlich-Peterson and Liu
635 isotherm equations as well as PFO, IPD, Elovich, and Avrami kinetic equations are also
636 indicated in some cases. The adsorption mechanism included a variety of interaction steps like
637 complexation, electrostatic attraction, precipitation, cation exchange, H-bonding, π - π interaction,
638 etc. The studied systems obeyed endothermic/ exothermic, spontaneous, and favorable natures.
639 NaOH and HCl were widely and efficiently applied as regenerating agents. For future prospects,
640 the practical application of wheat residues-based adsorbent against real wastewaters and the cost
641 analysis for the synthesis and utilization of these materials need to be considered. Moreover,

642 preparing other adsorbents from wheat residues like ash, silica, zeolite, etc. and exploring the
643 remediation of other pollutants like oils, surfactants, etc. are also need to be studied.

644 **References**

645 Ahmad T., M. Danish, 2018. Prospects of banana waste utilization in wastewater treatment: A
646 Review. *Journal of Environmental Management* 206, 330-348.

647 Ahmed M.J., M. Danish, I. Anastopoulos, K.O. Iwuozor, 2023. Recent progress on corn (*Zea*
648 *mays* L.)-based materials as raw, chemically modified, carbonaceous, and composite adsorbents
649 for aquatic pollutants: A review. *Journal of Analytical and Applied Pyrolysis* 172, 106004.

650 Akpomie K.G., Conradie J., 2023. Efficient adsorptive removal of paracetamol and thiazolyl
651 blue from polluted water onto biosynthesized copper oxide nanoparticles. *Sci. Rep.* 13, 1–15.

652 Al-Ghouti M.A., Al-Absi R.S., 2020. Mechanistic understanding of the adsorption and
653 thermodynamic aspects of cationic methylene blue dye onto cellulosic olive stones biomass from
654 wastewater. *Sci. Rep.* 10, 1–18.

655 Alrowais R., N. Said, M.T. Bashir, A. Ghazy, B. Alwushayh, M.M. Abdel Daiem, 2023.
656 Adsorption of diphenolic acid from contaminated water onto commercial and prepared activated
657 carbons from wheat straw. *Water* 15, 555.

658 Alzaydien A.S., 2015. Adsorption behavior of methyl orange onto wheat bran: Role of surface
659 and pH. *Oriental Journal of Chemistry* 31(2), 643-651.

660 Aliabadi H.M., Saberikhah E., Pirbazari A.E., Khakpour R., Alipour H., 2018.
661 Triethoxysilylpropylamine modified alkali treated wheat straw: An efficient adsorbent for methyl
662 orange adsorption. *Cellulose Chemistry and Technology* 52 (1-2), 129-140.

- 663 Albatrni H., H. Qiblawey, M.J. Al-Marri, 2022. Walnut shell based adsorbents: A review study
664 on preparation, mechanism, and application. *Journal of Water Process Engineering* 45, 102527.
- 665 Ali S., S. Noureen, M.B. Shakoor, M.Y. Haroon, M. Rizwan, A. Jilani, M.S. Arif, U. Khalil,
666 2020. Comparative evaluation of wheat straw and press mud biochars for Cr(VI) elimination
667 from contaminated aqueous solution. *Environmental Technology & Innovation* 19, 101017.
- 668 Ambika S., Kumar M., Pisharody L., Malhotra M., Kumar G., Sreedharan V., Singh L.,
669 Nidheesh P. V., Bhatnagar A., 2022. Modified biochar as a green adsorbent for removal of
670 hexavalent chromium from various environmental matrices: Mechanisms, methods, and
671 prospects. *Chem Eng J.* 439, 135716.
- 672 Ammar M.K., R.S. Hanafi, M.A. Choucry, H. Handoussa, 2023. Structural, functional,
673 nutritional composition and analytical profiling of *Triticum aestivum* L. *Applied Biological*
674 *Chemistry* 66, 48.
- 675 Ameri E., Z. Azizi-Haghigha, A. Mohe, 2014. Wheat straw as low cost adsorbent for Pb(II)
676 removal: Adsorption and equilibrium. *The 8th International Chemical Engineering Congress &*
677 *Exhibition (IChEC 2014) Kish, Iran, 24-27 February.*
- 678 Anastopoulos I., M.J. Ahmed, E.H. Hummadi, 2022. Eucalyptus-based materials as adsorbents
679 for heavy metals and dyes removal from (waste)waters. *Journal of Molecular Liquids* 356,
680 118864.
- 681 Anis M., S. Haydar, A.J. Bari, 2013. Adsorption of lead and copper from aqueous solution using
682 unmodified wheat straw. *Environmental Engineering and Management Journal* 12(11), 2117-
683 2124.

- 684 Aryee A.A., F.M. Mpatani, A.N. Kani, E. Dovi, R. Han, Z. Li, L. Qu, 2021. A review on
685 functionalized adsorbents based on peanut husk for the sequestration of pollutants in wastewater:
686 Modification methods and adsorption study. *Journal of Cleaner Production* 310, 127502.
- 687 Ata S., M.I. Din, A. Rasool, I. Qasim, I. UIMohsin, 2012. Equilibrium, thermodynamics, and
688 kinetic sorption studies for the removal of Coomassie brilliant blue on wheat bran as a low-cost
689 adsorbent. *Journal of Analytical Methods in Chemistry* Volume 2012, Article ID 405980, 8
690 pages doi:10.1155/2012/405980.
- 691 Bandara T., Xu J., Potter I. D., Franks A., Chaturika J. B. A. J., Tang C., 2020. Mechanisms for
692 the removal of Cd(II) and Cu(II) from aqueous solution and mine water by biochars derived from
693 agricultural wastes. *Chemosphere* 254, 126745.
- 694 Banerjee S., Chattopadhyaya M.C., Uma Sharma Y.C., 2014. Adsorption characteristics of
695 modified wheat husk for the removal of a toxic dye, methylene blue, from aqueous solutions.
696 *Journal of Hazardous, Toxic, and Radioactive Waste* 18(1), 56-63.
- 697 Banerjee S., R.K. Gautam, A. Jaiswal, P.K. Gautam, M.C. Chattopadhyaya, 2016. Study on
698 adsorption behavior of acid orange 10 onto modified wheat husk. *Desalination and Water*
699 *Treatment* 57(26), 12302-12315.
- 700 Baskar A.V., Bolan N., Hoang S.A., Sooriyakumar P., Kumar M., Singh L., Jasemizad T.,
701 Padhye L.P., Singh G., Vinu A., Sarkar B., Kirkham M.B., Rinklebe J., Wang S., Wang H.,
702 Balasubramanian R., Siddique K.H.M., 2022. Recovery, regeneration and sustainable
703 management of spent adsorbents from wastewater treatment streams: A review. *Science of The*
704 *Total Environment* 822, 153555.

- 705 Ben'koa E.M., V.V. Lunina, 2018. Adsorption of methylene blue on lignocellulosic plant
706 materials, *Russian Journal of Physical Chemistry A* 92(9) 1794–1798.
- 707 Bhavana B.K., S.N. Mudliar, S. Debnath, 2023. Life cycle assessment of fermentative xylitol
708 production from wheat bran: A comparative evaluation of sulphuric acid and chemical-free wet
709 air oxidation-based pretreatment. *Journal of Cleaner Production* 423, 138666.
- 710 Bogusz A., K. Nowak, M. Stefaniuk, R. Dobrowolski, P. Oleszczuk, 2017. Synthesis of biochar
711 from residues after biogas production with respect to cadmium and nickel removal from
712 wastewater. *Journal of Environmental Management* 201, 268–276.
- 713 Cao Y., W. Xiao, G. Shen, G. Ji, Y. Zhang, C. Gao, L. Han, 2019a. Carbonization and ball
714 milling on the enhancement of Pb(II) adsorption by wheat straw: Competitive effects of ion
715 exchange and precipitation. *Bioresource Technology* 273, 70–76.
- 716 Cao Y., G. Shen, Y. Zhang, C. Gao, Y. Li, P. Zhang, W. Xiao, L. Han, 2019b. Impacts of
717 carbonization temperature on the Pb(II) adsorption by wheat straw-derived biochar and related
718 mechanism. *Science of the Total Environment* 692, 479–489.
- 719 Chung W.J., J. Shim, B. Ravindran, 2022. Application of wheat bran based biomaterials and
720 nano-catalyst in textile wastewater. *Journal of King Saud University – Science* 34, 101775.
- 721 Chanajaree R., Sriuttha M., Lee V.S., Wittayanarakul K., 2021. Thermodynamics and kinetics of
722 cationic/anionic dyes adsorption on cross-linked chitosan. *J. Mol. Liq.* 322, 114507.
- 723 Chen S., Q. Yue, B. Gao, X. Xu, 2010. Equilibrium and kinetic adsorption study of the
724 adsorptive removal of Cr(VI) using modified wheat residue. *Journal of Colloid and Interface
725 Science* 349, 256–264.

- 726 Chen Y., Q. Chen, H. Zhao, J. Dang, R. Jin, W. Zhao, Y. Li, 2020a. Wheat straws and corn
727 straws as adsorbents for the removal of Cr(VI) and Cr(III) from aqueous solution: Kinetics,
728 isotherm, and mechanism. *ACS Omega* 5, 6003–6009.
- 729 Chen D., X. Wang, X. Wang, K. Feng, J. Su, J. Dong, 2020b. The mechanism of cadmium
730 sorption by sulphur-modified wheat straw biochar and its application cadmium-contaminated
731 soil. *Science of the Total Environment* 714, 136550.
- 732 Chen W.H., Hoang A.T., Nižetić S., Pandey A., Cheng C.K., Luque R., Ong H.C., Thomas S.,
733 Nguyen X.P., 2022. Biomass-derived biochar: From production to application in removing heavy
734 metal-contaminated water. *Process Safety and Environmental Protection* 160, 704-733.
- 735 Coelho G.F., A.C. Gonçalves Jr., J.C. Novoa-Muñoz, D. Fernandez-Calviño, M. Arias-
736 Estevez, M.J. Fernandez-Sanjurjo, E. Alvarez-Rodríguez, A. Núñez-Delgado, 2016.
737 Competitive and non-competitive cadmium, copper and lead sorption/desorption on wheat straw
738 affecting sustainability in vineyards. *Journal of Cleaner Production* 139, 1496-1503.
- 739 Deng J., Z. Zhai, Q. Yuan, G. Li, 2019. Effect of solution pH on adsorption of cefradine by
740 wheat straw and thermodynamic analysis. *Nature Environment and Pollution Technology* 18(1),
741 317-321.
- 742 Dhami D., P.L. Homagai, 2020. Adsorptive removal of malachite green dye from aqueous
743 solution using chemically modified charred and xanthated wheat bran. *Journal of Nepal
744 Chemical Society* 41(1), 103-109.

- 745 Dong J., Y. Du, R. Duyu, Y. Shang, S. Zhang, R. Han, 2019. Adsorption of copper ion from
746 solution by polyethylenimine modified wheat Straw. *Bioresource Technology Reports* 6, 96–
747 102.
- 748 Dutta A., Y. Diao, R. Jain, E.R. Rene, S. Dutta, 2016. Adsorption of cadmium from aqueous
749 solutions onto coffee grounds and wheat straw: Equilibrium and kinetic study. *Journal of*
750 *Environmental Engineering (American Society of Civil Engineers)* 142(9), 1-6.
- 751 Farooq U., M.A. Khan, M. Athar, J.A. Kozinski, 2011. Effect of modification of environmentally
752 friendly biosorbent wheat (*Triticum aestivum*) on the biosorptive removal of cadmium(II) ions
753 from aqueous solution. *Chemical Engineering Journal* 171, 400– 410.
- 754 Farooq U., J. A. Kozinski, M. A. Khan, M. Athar, 2010. Biosorption of heavy metal ions using
755 wheat based biosorbents – A review of the recent literature. *Bioresource Technology* 101, 5043–
756 5053.
- 757 Filippini T., Wise L.A., Vinceti M., 2022. Cadmium exposure and risk of diabetes and
758 prediabetes: a systematic review and dose-response meta-analysis. *Environ Int* 158, 106920.
- 759 Foong S.Y., Y.H. Chan, B.L.F. Chin, S.S.M. Lock, C.Y. Yee, C.L. Yiin, W. Peng , S.S. Lam,
760 2022. Production of biochar from rice straw and its application for wastewater remediation - An
761 overview. *Bioresource Technology* 360, 127588.
- 762 Franco D., L.F.O. Silva, K. da Boit Martinello, J.C. Diel, J. Georgin, M.S. Netto, H.A. Pereira,
763 E.C. Lima, G.L. Dotto, 2021. Transforming agricultural waste into adsorbent: application of
764 *Fagopyrum esculentum* wheat husks treated with H_2SO_4 to adsorption of the 2,4-D herbicide.
765 *Journal of Environmental Chemical Engineering* 9, 106872.

- 766 Fricler V.Y., G.S. Nyashina , K.Yu. Vershinina , K.V. Vinogradskiy , A.S. Shvets , P.A.
767 Strizhak, 2023. Microwave pyrolysis of agricultural waste: Influence of catalysts, absorbers,
768 particle size and blending components. *Journal of Analytical and Applied Pyrolysis* 171, 105962.
- 769 Fu H., Ma S., Xu S., Duan R., Cheng G., Zhao P., 2021. Hierarchically porous magnetic biochar
770 as an efficient amendment for cadmium in water and soil: Performance and mechanism.
771 *Chemosphere* 281, 130990.
- 772 Gorgievski M., D. Božić, V. Stanković, N. Štrbac, S. Šerbula, 2013. Kinetics, equilibrium and
773 mechanism of Cu^{2+} , Ni^{2+} and Zn^{2+} ions biosorption using wheat straw. *Ecological Engineering*
774 58, 113– 122.
- 775 Guo Y., W. Zhu, G. Li, X. Wang, L. Zhu, 2016. Effect of alkali treatment of wheat straw on
776 adsorption of Cu(II) under acidic condition. *Journal of Chemistry* Volume 2016, Article ID
777 6326372, 10 pages, <http://dx.doi.org/10.1155/2016/6326372>.
- 778 Habiba U., S. Mutahir, M.A. Khan , M. Humayun , M.S. Refat, K.S. Munawar, 2022. Effective
779 removal of refractory pollutants through cinnamic acid-modified wheat husk biochar:
780 Experimental and DFT-Based Analysis. *Catalysts* 12, 1063.
- 781 Haghghat Z.A., E. Ameri, 2016. Synthesis and characterization of nano magnetic wheat straw
782 for lead adsorption. *Desalination and Water Treatment* 57(21), 9813-9823.
- 783 Hamid Y., Liu L., Usman M., Naidu R., Haris M., Lin Q., 2022. Functionalized biochars:
784 Synthesis, characterization, and applications for removing trace elements from water. *J. Hazard.*
785 *Mater.* 437,129337.

- 786 Han R., Zhang L., Song C., Zhang M., Zhu H., Zhang L., 2010. Characterization of modified
787 wheat straw, kinetic and equilibrium study about copper ion and methylene blue adsorption in
788 batch mode. *Carbohydrate Polymers* 79(4), 1140-1149.
- 789 Haq H.A., T. Javed, M.A. Abid, S. Zafar, M.I. Din, 2021. Adsorption of Crystal violet dye from
790 synthetic textile effluents by utilizing wheat bran (*Triticum aestivum*). *Desalination and Water
791 Treatment* 224, 395–406.
- 792 Haris M., Hamid Y., Usman M., Wang L., Saleem A., Su F., Guo J., Li Y., 2021. Crop residues
793 derived biochar: synthesis, properties, characterization and application for the removal of trace
794 elements in soils. *J. Hazard. Mater.* 416, 126212.
- 795 Haris M., Usman M., Su F., Lei W., Saleem A., Hamid Y, Guo J., Li Y., 2022. Programmable
796 synthesis of exfoliated biochar nanosheets for selective and highly efficient adsorption of
797 thallium. *Chem. Eng. J.* 434, 134842.
- 798 Hassanein T.F., B. Koumanova, 2010. Evaluation of adsorption potential of the agricultural
799 waste wheat straw for basic yellow 21. *Journal of the University of Chemical Technology and
800 Metallurgy* 45(4) 407-414.
- 801 Hou Q., W. Li, M. Ju, L. Liu, Y. Chen, Q. Yang, J. Wang, 2015. Separation of polysaccharides
802 from rice husk and wheat bran using solvent system consisting of BMIMOA_c and DMI.
803 *Carbohydrate Polymers* 133, 517–523.
- 804 Huang Z., X. Fang, S. Wang, N. Zhou, S. Fan, 2023. Effects of KMnO₄ pre- and post-treatments
805 on biochar properties and its adsorption of tetracycline. *Journal of Molecular Liquids* 373,
806 121257.

- 807 Ighalo J.O., J. Conradie, C.R. Ohoro, J.F. Amaku, K.O. Oyedotun, N. W. Maxakato, K.G.
808 Akpomie, E.S. Okeke, C. Olisah, A. Malloum, K.A. Adegoke, 2023. Biochar from coconut
809 residues: An overview of production, properties, and applications. *Industrial Crops & Products*
810 204, 117300.
- 811 Iwuozor K.O., Emenike E.C., Aniagor C.O., Iwuchukwu F.U., Ibitogbe E.M., Temitayo O.B.,
812 Omuku P.E., Adeniyi A.G., 2022. Removal of pollutants from aqueous media using cow dung-
813 based adsorbents. *Current Research in Green and Sustainable Chemistry* 5, 100300.
- 814 Jamil U., M. Zeeshan, S.R. Khan, S. Saeed, 2023. Synthesis and two-step KOH based activation
815 of porous biochar of wheat straw and waste tire for adsorptive exclusion of chromium (VI) from
816 aqueous solution; thermodynamic and regeneration study. *Journal of Water Process Engineering*
817 53, 103892.
- 818 James A., D. Yadav, 2021. Valorization of coconut waste for facile treatment of contaminated
819 water: A comprehensive review (2010–2021). *Environmental Technology & Innovation* 24,
820 102075.
- 821 Jiang D., S. Lv, D. Jiang, H. Xu, H. Kang, X. Song, S. He, 2023. Effect of modification methods
822 on water absorption and strength of wheat straw fiber and its cement-based composites. *Journal*
823 *of Building Engineering* 71, 106466.
- 824 Kalderis D., A. Seifi, T.K. Trang, T. Tsubota, I. Anastopoulos, I. Manariotis, I. Pashalidis, A.
825 Khataee, 2023. Bamboo-derived adsorbents for environmental remediation: A review of recent
826 progress. *Environmental Research* 224, 115533.

- 827 Kaya K., E. Pehlivan, C. Schmidt, M. Bahadir, 2014. Use of modified wheat bran for the
828 removal of chromium(VI) from aqueous solutions. *Food Chemistry* 158, 112–117.
- 829 Khan M.H., N.M. Akash, S. Akter, M. Rukh, C. Nzediegwu , M.S. Islam, 2023. A
830 comprehensive review of coconut-based porous materials for wastewater treatment and CO₂
831 capture. *Journal of Environmental Management* 338, 117825.
- 832 Khan T.S., U. Mubeen, 2012. Wheat straw: A pragmatic overview. *Current Research Journal of*
833 *Biological Sciences* 4(6) 673-675.
- 834 Kohzadi S., N. Marzban, J.A. Libra, M. Bundschuh, A. Maleki, 2023. Removal of RhB from
835 water by Fe-modified hydrochar and biochar – An experimental evaluation supported by genetic
836 programming. *Journal of Molecular Liquids* 369, 120971.
- 837 Kumar R., O. Prakash, 2023. Experimental investigation on effect of season on the production of
838 bioethanol from wheat-stalk (WS) using simultaneous saccharification and fermentation (SSF)
839 method. *Fuel* 351, 128958.
- 840 Kwak J.-H., M.S. Islam , S. Wang, S.A. Messele, M. Anne Naeth, M. Gamal El-Din, S.X.
841 Chang, 2019. Biochar properties and lead(II) adsorption capacity depend on feedstock type,
842 pyrolysis temperature, and steam activation. *Chemosphere* 231, 393-404.
- 843 Laidani Y., G. Henini, S. Hanini, A. Fekaoui, 2019. Studies of the biosorption of textile dye
844 onto wheat straw. *Scientific Study & Research Chemistry & Chemical Engineering,*
845 *Biotechnology, Food Industry* 20 (4), 609 – 625.

- 846 Li W.-G., W. Zhao, H.-M. Liu, L. Ao, K.-S. Liu, Y.-S. Guan, S.-F. Zai, S.-L. Chen, Z.-M. Zong,
847 X.-Y. Wei, 2018. Supercritical ethanolysis of wheat stalk over calcium oxide. *Renewable Energy*
848 120, 300–305.
- 849 Li Y., X. Zhang, P. Zhang, X. Liu, L. Han, 2020. Facile fabrication of magnetic bio-derived
850 chars by co-mixing with Fe₃O₄ nanoparticles for effective Pb²⁺ adsorption: Properties and
851 Mechanism. *Journal of Cleaner Production* 262, 121350.
- 852 Li H., M. Zhou, E. Guan, Z. Li, 2021. Preparation of wheat bran-titanium dioxide (TiO₂)
853 composite and its application for selenium adsorption. *Journal of Cereal Science* 99, 103230.
- 854 Li H., J. Kong, H. Zhang, J. Gao, Y. Fang, J. Shi, T. Ge, T. Fang, Y. Shi, R. Zhang, N. Zhang, X.
855 Dong, Y. Zhang, H. Li, 2023. Mechanisms and adsorption capacities of ball milled biomass fly
856 ash/biochar composites for the adsorption of methylene blue dye from aqueous solution. *Journal*
857 *of Water Process Engineering* 53, 103713.
- 858 Lin Q., K. Wang, M. Gao, Y. Bai, L. Chen, H. Ma, 2017. Effectively removal of cationic and
859 anionic dyes by pH-sensitive amphoteric adsorbent derived from agricultural waste-wheat straw.
860 *Journal of the Taiwan Institute of Chemical Engineers* 76, 65–72.
- 861 Liu J., H. Wang, N. Ma, B. Zhou, H. Chen, R. Yuan, 2022a. Optimization of the raw materials of
862 biochars for the adsorption of heavy metal ions from aqueous solution. *Water Science &*
863 *Technology* 85(10), 2869-2881.
- 864 Liu Z.-T., Shao J., Li Y., Wu Y.-R., An Y., Sun Y.-F., Fei Z.-H., 2022b. Adsorption performance
865 of tetracycline in water by alkali-modified wheat straw biochars. *China Environmental Science*
866 42(8), 3736–3743.

- 867 Liu Y., X. Zhao, D. Ma, Y. Li, R. Han, 2012. Adsorption of copper (II) from solution by wheat
868 husk in batch mode. *Advanced Materials Research* 393-395, 1093-1097.
- 869 Lu X., Liu X., Zhang W., Wang X., Wang S., Xia T., 2020. The residue from the acidic
870 concentrated lithium bromide treated crop residue as biochar to remove Cr (VI). *Bioresour. Tech.*
871 296, 122348.
- 872 Ma Z., Q. Li, Q. Yue, B. Gao, W. Li, X. Xu, Q. Zhong, 2011. Adsorption removal of ammonium
873 and phosphate from water by fertilizer controlled release agent prepared from wheat straw.
874 *Chemical Engineering Journal* 171, 1209– 1217.
- 875 Mehdinejadiani B., S.M. Amininasab, L. Manhooei, 2019. Enhanced adsorption of nitrate from
876 water by modified wheat straw: equilibrium, kinetic and thermodynamic studies. *Water Science
877 & Technology* 79.2, 302-313.
- 878 Mirjalili M., Tabatabai M.B., Karimi L., 2011. Novel herbal adsorbent based on wheat husk for
879 reactive dye removal from aqueous solutions. *African Journal of Biotechnology* 10, 14478–
880 14484.
- 881 Mo J., Q. Yang, N. Zhang, W. Zhang, Y. Zheng, Z. Zhang, 2018. A review on agro-industrial
882 waste (AIW) derived adsorbents for water and wastewater treatment. *Journal of Environmental
883 Management* 227, 395–405.
- 884 Mohite A.S., A.R. Jagtap, M.S. Avhad, A. P. More, 2022. Recycling of major agriculture crop
885 residues and its application in polymer industry: A review in the context of waste to energy
886 nexus. *Energy Nexus* 7, 100134.

- 887 Mohamed M.I., A.A. Sabri, E.J. Taha, 2019. Application of wheat husk in color removal of
888 textile wastewater. *Engineering and Technology Journal* 37, Part C, No. 2.
- 889 Mohammadi L., Baniasadi M., Rahdar A., Kyzas G.Z., 2021. Removal of acid dye from aqueous
890 solutions with adsorption onto modified wheat bran – modeling with artificial neural networks.
891 *Biointerface Research in Applied Chemistry* 11, 14044–14056.
- 892 Mu RM, M X Wang, QW Bu, D Liu, YL Zhao, 2018a. Adsorption of Pb(II) from aqueous
893 solutions by wheat straw biochar. *IOP Conf. Series: Earth and Environmental Science* 191,
894 012041.
- 895 Mu R., M. Wang, Q. Bu, D. Liu, Y. Zhao, 2018b. Improving lead adsorption through chemical
896 modification of wheat straw by lactic acid. *IOP Conf. Series: Earth and Environmental Science*
897 108, 022063.
- 898 Muhammad H., Wei T., Cao G., Yu S.H., Ren X.H., Jia H.L., 2021. Study of soil
899 microorganisms modified wheat straw and biochar for reducing cadmium leaching potential and
900 bioavailability. *Chemosphere*. 273, 129644.
- 901 Nzediegwu C., M. Anne Naeth, S.X. Chang, 2021. Lead(II) adsorption on microwave-pyrolyzed
902 biochars and hydrochars depends on feedstock type and production temperature. *Journal of*
903 *Hazardous Materials* 412, 125255.
- 904 Ogata F., Y. Uematsu, N. Nagai, M. Nakamura, A. Tabuchi, C. Saenjum, T. Nakamura, N.
905 Kawasaki, 2022. Wheat brans as waste biomass based on a potential bio-adsorbent for removing
906 platinum(IV) ions from aqueous phase. *Bioresource Technology Reports* 20, 101238.

- 907 Ogata F., N. Nagai, R. Itami, T. Nakamura, N. Kawasaki, 2020. Potential of virgin and calcined
908 wheat bran biomass for the removal of chromium(VI) ion from a synthetic aqueous solution.
909 *Journal of Environmental Chemical Engineering* 8, 103710.
- 910 Ogata F., T. Nakamura, N. Kawasaki, 2018. Adsorption capability of virgin and calcined wheat
911 bran for molybdenum present in aqueous solution and elucidating the adsorption mechanism by
912 adsorption isotherms, kinetics, and regeneration. *Journal of Environmental Chemical*
913 *Engineering* 6, 4459–4466.
- 914 Ogata F., M. Kangawa, Y. Iwata, A. Ueda, Y. Tanaka, N. Kawasaki, 2014. A Study on the
915 adsorption of heavy Metals by Using Raw Wheat Bran Bioadsorbent in Aqueous Solution.
916 *Phase, Chem. Pharm. Bull.* 62(3) 247–253.
- 917 Othmani A., Magdoui S., Kumar P.S., Kapoor A., Chellam P.V., Gökkuş Ö., 2022. Agricultural
918 waste materials for adsorptive removal of phenols, chromium (VI) and cadmium (II) from
919 wastewater: A review. *Environmental Research* 204, 111916.
- 920 Pirbazari A.E., E. Saberikhah, N.G. Ahmadgurabi, 2016. Study of isotherm and kinetics
921 parameters for methylene blue adsorption onto wheat straw. *International Academic Journal of*
922 *Science and Engineering* 3(4), 132-136.
- 923 Pirbazari A.E., E. Saberikhah, S.S.H. Kozani, 2014. Fe₃O₄-wheat straw: preparation,
924 characterization and its application form ethylene blue adsorption. *Water Resources and*
925 *Industry* 7-8, 23–37.
- 926 Plazinski W., Rudzinski W., Plazinska A., 2009. Theoretical Models of Sorption Kinetics
927 Including a Surface Reaction Mechanism: A Review. *Adv. Colloid Interface Sci.* 152, 2–13.

- 928 Pan W., H. Xie, Y. Zhou, Q. Wu, J. Zhou, X. Guo, 2023. Simultaneous adsorption removal of
929 organic and inorganic phosphorus from discharged circulating cooling water on biochar derived
930 from agricultural waste. *Journal of Cleaner Production* 383, 135496.
- 931 Qi G., Z. Pan, X. Zhang, S. Chang, H. Wang, M. Wang, W. Xiang, B. Gao, 2023. Microwave
932 biochar produced with activated carbon catalyst: Characterization and adsorption of heavy
933 metals. *Environmental Research* 216, 114732.
- 934 Rani P., M. Bansal, V.V. Pathak, 2022. Experimental and kinetic studies for improvement of
935 biogas production from KOH pretreated wheat straw. *Current Research in Green and Sustainable
936 Chemistry* 5, 100283.
- 937 Rasouli A., A. Bafkar, Z. Chaghakaboodi, 2020. Kinetic and equilibrium studies of adsorptive
938 removal of sodium-ion onto wheat straw and rice husk wastes. *Central Asian Journal of
939 Environmental Science and Technology Innovation* 1(6), 310-329.
- 940 Rashid R., I. Shafiq, P. Akhter, M.J. Iqbal, M. Hussain, 2021. A state-of-the-art review on
941 wastewater treatment techniques: the effectiveness of adsorption method. *Environmental Science
942 and Pollution Research* 28, 9050–9066.
- 943 Rout D.R., H.M. Jena, O. Baigenzhenov, A. Hosseini-Bandegharai, 2023. Graphene-based
944 materials for effective adsorption of organic and inorganic pollutants: A critical and
945 comprehensive review. *Science of the Total Environment* 863, 160871.
- 946 Sabah I., A. I. Alward, 2019. Adsorption of Congo red dye from aqueous solutions by wheat
947 husk. *Journal of Engineering* 25(12), 72-84.

- 948 Sarrai A.E., Y. Belaissa, R. Kirdi, S. Hanini, T. Szabó, L. Nagy, 2022. Modeling and
949 optimization of Tylosin adsorption using dehydrated wheat bran: adsorption behaviors, kinetic
950 and thermodynamic studies. *Reaction Kinetics, Mechanisms and Catalysis* 135, 1905–1928.
- 951 Saleem A., Chen J., Liu M., Liu N., Usman M., Wang K., Haris M., Zhang Y., Li P., 2023.
952 Versatile magnetic mesoporous carbon derived nano-adsorbent for synchronized toxic metal
953 removal and bacterial disinfection from water matrices. *Small* 19(5), 2207348.
- 954 Sinha R., Kumar R., Sharma P., Kant N., Shang. J, Aminabhavi T.M., 2022. Removal of
955 hexavalent chromium via biochar-based adsorbents: State-of-the-art, challenges, and future
956 perspectives. *J. Environ. Manage.* 317, 115356.
- 957 Shamsollahi Z., A. Partovinia, 2019. Recent advances on pollutants removal by rice husk as a
958 bio-based adsorbent: A critical review. *Journal of Environmental Management* 246, 314–323.
- 959 Shahaji S.P., C.S. Tanaji, J.A. Suhas, 2023. Removal of nitrate from aqueous solution by using
960 orange peel and wheat straw. *Materials Today: Proceedings* 73, 468–473.
- 961 Shi W., H. Wang, J. Yan, L. Shan, G. Quan, X. Pan, L. Cui, 2022a. Wheat straw derived biochar
962 with hierarchically porous structure for bisphenol A removal: Preparation, characterization, and
963 adsorption properties. *Separation and Purification Technology* 289, 120796.
- 964 Shi Q., S. Zhang, M. Xie, C. Christodoulatos, X. Meng, 2022b. Competitive adsorption of
965 nitrate, phosphate, and sulfate on amine-modified wheat straw: In-situ infrared spectroscopic and
966 density functional theory study. *Environmental Research* 215, 114368.

- 967 Shen Z., Y. Zhang, O. McMillan, F. Jin, A. Al-Tabbaa, 2017. Characteristics and mechanisms of
968 nickel adsorption on biochars produced from wheat straw pellets and rice husk. *Environ. Sci.*
969 *Pollut. Res.* 24, 12809–12819
- 970 Shen T., P. Wang, L. Hu, Q. Hu, X. Wang, G. Zhang, 2021. Adsorption of 4-chlorophenol by
971 wheat straw biochar and its regeneration with persulfate under microwave irradiation. *Journal of*
972 *Environmental Chemical Engineering* 9, 105353.
- 973 Shou J., M. Qiu, 2016. Adsorption kinetics of phenol in aqueous solution onto activated carbon
974 from wheat straw lignin. *Desalination and Water Treatment* 57:7, 3119-3124.
- 975 Solangi N.H., J. Kumar, S.A. Mazari, S. Ahmed, N. Fatima, N.M. Mubarak, 2021. Development
976 of fruit waste derived bio-adsorbents for wastewater treatment: A review. *Journal of Hazardous*
977 *Materials* 416, 125848.
- 978 Sodkouieh S.M., M. Kalantari, T. Shamspur, 2023. Methylene blue adsorption by wheat straw-
979 based adsorbents: Study of adsorption kinetics and isotherms. *Korean J. Chem. Eng.*, 40(4), 873-
980 881.
- 981 Suresh A., G. Rahul, N. Sai Akhil, A. Rithwik Reddy, P.L. Bharath Sai, C. Sairam Reddy, 2022.
982 Transformation of crop residual waste into fertilizer for farmers: As an alternative to crop
983 residual burning. *Materials Today: Proceedings* 64, 230–238.
- 984 Tan X., B. Gao, X. Xu, Y. Wang, J. Ling, Q. Yue, Q. Li, 2012. Perchlorate uptake by wheat
985 straw based adsorbent from aqueous solution and its subsequent biological regeneration.
986 *Chemical Engineering Journal* 211–212, 37–45.

- 987 Tefera M., M. Tulu, 2021. Preparation and characterization of activated carbon from wheat straw
988 to remove 2, 4-dichlorophenoxy acetic acid from aqueous solutions. *Current Chemistry Letters*
989 10, 175–186.
- 990 Tian Y., M. Wu, X. Lin, P. Huang, Y. Huang, 2011. Synthesis of magnetic wheat straw for
991 arsenic adsorption. *Journal of Hazardous Materials* 193, 10– 16.
- 992 Tokula B.E., A.O. Dada, A.A. Inyinbor, K.S. Obayomi, O.S. Bello, U. Pal, 2023. Agro-waste
993 based adsorbents as sustainable materials for effective adsorption of Bisphenol A from the
994 environment: A review. *Journal of Cleaner Production* 388, 135819.
- 995 Trivedi A.K., A. Kumar, M.K. Gupta, 2023. Extraction of nanocellulose from wheat straw and
996 its characterization. *Materials Today: Proceedings* 78, 48–54.
- 997 Vasu D., S. Kumar, Y.K. Walia, 2019. Removal of dyes using wheat husk waste as a low-cost
998 adsorbent. *Environmental Claims Journal* 32(1), 67-76.
- 999 Wang X., Y. Zhao, J. Deng , Y. Zhou, S. Yuan, 2023a. Study on the influence mechanism of
1000 mineral components in biochar on the adsorption of Cr(VI). *Fuel* 340, 127631.
- 1001 Wang H., J. Dai, H. Chen, F. Wang, Y. Zhu, J. Liu, B. Zhou, R. Yuan, 2023. Adsorption of
1002 phosphate by Mg/Fe-doped wheat straw biochars optimized using response surface
1003 methodology: Mechanisms and application in domestic sewage. *Environ. Eng. Res.* 28(2),
1004 210602.
- 1005 Wang Y., K. Zheng, Z. Jiao, W. Zhan, S. Ge, S. Ning, S. Fang, X. Ruan, 2022. Simultaneous
1006 removal of Cu^{2+} , Cd^{2+} and Pb^{2+} by modified wheat straw biochar from aqueous solution:
1007 Preparation, characterization and adsorption mechanism. *Toxics* 10(6), 316.

- 1008 Wang J., X. Liu, M. Yang, H. Han, S. Zhang, G. Ouyang, R. Han, 2021. Removal of tetracycline
1009 using modified wheat straw from solution in batch and column modes. *Journal of Molecular*
1010 *Liquids* 338, 116698.
- 1011 Wang S., S. Ai, C. Nzediegwu, J.-H. Kwak, M.S. Islamd, Y. Li, S.X. Chang, 2020. Carboxyl and
1012 hydroxyl groups enhance ammonium adsorption capacity of iron (III) chloride and hydrochloric
1013 acid modified biochars. *Bioresource Technology* 309, 123390.
- 1014 Wang L., Wang Y., Ma F., Tankpa V., Bai S., Guo X., Wang X., 2019. Mechanisms and
1015 reutilization of modified biochar used for removal of heavy metals from wastewater: A review.
1016 *Sci of the Total Environ* 668, 1298–1309.
- 1017 Wang P., Y. Yin, Y. Guo, C. Wang, 2016. Preponderant adsorption for chlorpyrifos over atrazine
1018 by wheat straw-derived biochar: experimental and theoretical studies. *RSC Adv.*6, 10615–10624.
- 1019 Wang X.S., Z.P. Lu, H.H. Miao, W. He, H.L. Shen, 2011. Kinetics of Pb (II) adsorption on black
1020 carbon derived from wheat residue. *Chemical Engineering Journal* 166, 986–993.
- 1021 Wang X.S., L.F. Chen, F.Y. Li, K.L. Chen, W.Y. Wan, Y.J. Tang, 2010. Removal of Cr (VI)
1022 with wheat-residue derived black carbon: Reaction mechanism and adsorption performance.
1023 *Journal of Hazardous Materials* 175, 816–822.
- 1024 Wu M., H. Liu, C. Yang, 2019. Effects of pretreatment methods of wheat straw on adsorption of
1025 Cd(II) from waterlogged paddy soil. *Int. J. Environ. Res. Public Health* 16, 205.
- 1026 Xiao W., R. Sun , S. Hu , C. Meng , B. Xie , M. Yi , Y. Wu, 2023. Recent advances and future
1027 perspective on lignocellulose-based materials as adsorbents in diverse water treatment
1028 applications. *International Journal of Biological Macromolecules* 253, 126984.

- 1029 Xiang W., X. Zhang, J. Luo, Y. Li, T. Guo, B. Gao, 2022. Performance of lignin impregnated
1030 biochar on tetracycline hydrochloride adsorption: Governing factors and mechanism.
1031 *Environmental Research* 215, 114339.
- 1032 Xing J., C. Chen, J. Qiu, X. Sun, 2013. Adsorption of lead ion from aqueous solution using
1033 acetic acid modified wheat bran. *J. Indian Chem. Soc.* 90, 2217-2222.
- 1034 Xu X., B.-Y. Gao, X. Tan, Q.-Y. Yue, Q.-Q. Zhong, Q. Li, 2011a. Characteristics of amine-
1035 crosslinked wheat straw and its adsorption mechanisms for phosphate and chromium (VI)
1036 removal from aqueous solution. *Carbohydrate Polymers* 84, 1054–1060.
- 1037 Xu X., Y. Gao, B. Gao, X. Tan, Y.-Q. Zhao, Q. Yue, Y. Wang, 2011b. Characteristics of
1038 diethylenetriamine-crosslinked cotton stalk/wheat stalk and their biosorption capacities for
1039 phosphate. *Journal of Hazardous Materials* 192, 1690– 1696.
- 1040 Xu J., Y. Zhang, B. Li, S. Fan, H. Xu, D.-X. Guan, 2022. Improved adsorption properties of
1041 tetracycline on KOH/KMnO₄ modified biochar derived from wheat straw. *Chemosphere* 296,
1042 133981.
- 1043 Yadav A.K., R. Abbassi, A. Gupta, M. Dadashzadeh, 2013. Removal of fluoride from aqueous
1044 solution and groundwater by wheat straw, sawdust and activated bagasse carbon of sugarcane.
1045 *Ecological Engineering* 52, 211– 218.
- 1046 Yafetto L., G.T. Odamtten, M. Wiafe-Kwagyan, 2023. Valorization of agro-industrial wastes
1047 into animal feed through microbial fermentation: A review of the global and Ghanaian case.
1048 *Heliyon* 9, e14814

- 1049 Yan J., X. Zuo, S. Yang, R. Chen, T. Cai, D. Ding, 2022. Evaluation of potassium ferrate
1050 activated biochar for the simultaneous adsorption of copper and sulfadiazine: Competitive versus
1051 synergistic. *Journal of Hazardous Materials* 424, 127435.
- 1052 Yaneva Z.L., Georgieva N.V., 2013. Removal of diazo dye from the aqueous phase by
1053 biosorption onto ball-milled maize cob (BMMC) biomass of *Zea mays*. *Macedonian Journal of*
1054 *Chemistry and Chemical Engineering* 32 (1), 133-149
- 1055 Yang F., L. Sun, W. Xie, Q. Jiang, Y. Gao, W. Zhang, Y. Zhang, 2017. Nitrogen-functionalization
1056 biochars derived from wheat straws via molten salt synthesis: An efficient adsorbent for atrazine
1057 removal. *Science of the Total Environment* 607–608, 1391–1399.
- 1058 Yang H.I., K. Lou, A.U. Rajapaksha, Y.S. Ok, A.O. Anyia, S.X. Chang, 2018. Adsorption of
1059 ammonium in aqueous solutions by pine sawdust and wheat straw biochars. *Environ. Sci. Pollut.*
1060 *Res.* 25, 25638–25647.
- 1061 Yang S.-S., Chen Y.-d., Kang J.-H., Xie T.-R., He L., Xing D.-F., Ren N.-Q., Ho S.-H., Wu W.-
1062 M., 2019. Generation of high-efficient biochar for dye adsorption using frass of yellow
1063 mealworms (larvae of *Tenebrio molitor* Linnaeus) fed with wheat straw for insect biomass
1064 production. *Journal of Cleaner Production* 227, 33-47.
- 1065 Yang W., T. Feng, M. Flury, B. Li, J. Shang, 2020. Effect of sulfamethazine on surface
1066 characteristics of biochar colloids and its implications for transport in porous media.
1067 *Environmental Pollution* 256, 113482.
- 1068 Yao S., H. Lai, Z. Shi, 2012. Biosorption of methyl blue onto tartaric acid modified wheat bran
1069 from aqueous solution. *Iranian Journal of Environmental Health Sciences & Engineering* 9:16.

- 1070 You H., Chen J., Yang C., Xu L., 2016. Selective removal of cationic dye from aqueous solution
1071 by low-cost adsorbent using phytic acid modified wheat straw. *Colloids and Surfaces A:
1072 Physicochemical and Engineering Aspects* 509, 91-98.
- 1073 Yuan Q., P. Wang, X. Wang, B. Hu, C. Wang, X. Xing, 2023. Nano-chlorapatite modification
1074 enhancing cadmium(II) adsorption capacity of crop residue biochars. *Science of the Total
1075 Environment* 865, 161097.
- 1076 Zama E.F., Zhu Y.G., Reid B.J., Sun G.X., 2017. The role of biochar properties in influencing
1077 the sorption and desorption of Pb(II), Cd(II) and As(III) in aqueous solution. *J. Clean Prod.* 148,
1078 127–136.
- 1079 Zhao Y., R. Zhang, H. Liu, M. Li, T. Chen, D. Chen, X. Zou, R.L. Frost, 2019. Green
1080 preparation of magnetic biochar for the effective accumulation of Pb (II): Performance and
1081 mechanism. *Chemical Engineering Journal* 375, 122011.
- 1082 Zhang W., H. Li, X. Kan, L. Dong, H. Yan, Z. Jiang, H. Yang, A. Li, R. Cheng, 2012.
1083 Adsorption of anionic dyes from aqueous solutions using chemically modified straw.
1084 *Bioresource Technology* 117, 40–47.
- 1085 Zhang R., J. Zhang, X. Zhang, C. Dou, R. Han, 2014a. Adsorption of Congo red from aqueous
1086 solutions using cationic surfactant modified wheat straw in batch mode: Kinetic and equilibrium
1087 study. *Journal of the Taiwan Institute of Chemical Engineers* 45, 2578–2583.
- 1088 Zhang X.N., Mao G.Y., Jiao Y.B., Shang Y., Han R.P., 2014b. Adsorption of anionic dye on
1089 magnesium hydroxide-coated pyrolytic bio-char and reuse by microwave irradiation. *Int. J.
1090 Environ. Sci. Technol.* 11, 1439–1448.

- 1091 Zhang Y., G. Huang, C. An, X. Xin, X. Liu, M. Raman, Y. Yao, W. Wang, M. Doble, 2017.
1092 Transport of anionic azo dyes from aqueous solution to Gemini surfactant-modified wheat bran:
1093 Synchrotron infrared, molecular interaction and adsorption studies. *Science of the Total*
1094 *Environment* 595, 723–732.
- 1095 Zhang J., M. Lu, J. Wan, Y. Sun, H. Lan, X. Deng, 2018a. Effects of pH, dissolved humic acid
1096 and Cu^{2+} on the adsorption of norfloxacin on montmorillonite-biochar composite derived from
1097 wheat straw. *Biochemical Engineering Journal* 130, 104–112.
- 1098 Zhang W.-X., L. Lai, P. Mei, Y. Li, Y.-H. Li, Y. Liu, 2018b. Enhanced removal efficiency of
1099 acid red 18 from aqueous solution using wheat bran modified by multiple quaternary ammonium
1100 salts. *Chemical Physics Letters* 710, 193–201.
- 1101 Zhang S., M.A.S. Abdalla, Z. Luo, S. Xia, 2018c. The wheat straw biochar research on the
1102 adsorption/desorption behaviour of mercury in wastewater. *Desalination and Water Treatment*
1103 112, 147–160.
- 1104 Zhang Y., X. Song, P. Zhang, H. Gao, C. Ou, X. Kong, 2020a. Production of activated carbons
1105 from four wastes via one-step activation and their applications in Pb^{2+} adsorption: Insight of ash
1106 content. *Chemosphere* 245, 125587.
- 1107 Zhang Z., Wang G., Li W., Zhang L., Chen T., Ding L., 2020b. Degradation of methyl orange
1108 through hydroxyl radical generated by optically excited biochar: Performance and mechanism.
1109 *Colloids and Surfaces A: Physicochemical and Engineering Aspects* 601,125034

1110 Zhang H., S. Tian, Y. Zhu, W. Zhong, R. Qiu, L. Han, 2022. Insight into the adsorption
1111 isotherms and kinetics of Pb (II) on pellet biochar via in-situ non-destructive 3D visualization
1112 using micro-computed tomography. *Bioresource Technology* 358, 127406.

1113 Zhang L., M. Feng, D. Zhao, M. Li, S. Qiu, M. Yuan, C. Guo, W. Han, K. Zhang, F. Wang,
1114 2023. La-Ca-quaternary amine-modified straw adsorbent for simultaneous removal of nitrate and
1115 phosphate from nutrient-polluted water. *Separation and Purification Technology* 304, 122248.

1116 Zhong Q.-Q., Q.-Y. Yue, B.-Y. Gao, Q. Li, X. Xu, 2013. A novel amphoteric adsorbent derived
1117 from biomass materials: Synthesis and adsorption for Cu(II)/Cr(VI) in single and binary systems.
1118 *Chemical Engineering Journal* 229, 90–98.

1119 Zhu N., Yan T., Qiao J., Cao H., 2016. Adsorption of arsenic, phosphorus and chromium by
1120 bismuth impregnated biochar: Adsorption mechanism and depleted adsorbent utilization.
1121 *Chemosphere*, 164, 32–40.

1122 **Figure Captions**

1123 **Fig. 1.** FTIR spectra of raw WS, NaOH modified MWS, and NaOH/monochloroacetic acid
1124 modified CMMWS wheat straws. (Reprinted with permission from Ref. (Sodkouieh et al., 2023).
1125 Copyright 2023 Springer).

1126 **Fig. 2.** SEM images of (a) wheat straw biochar WSBC (b) KOH activated biochar WSKOH_{dry}
1127 1:3. (Reprinted with permission from Ref. (Jamil et al., 2023). Copyright 2023 Elsevier).

1128 **Fig. 3.** Illustration of the potential mechanism of interaction between MB dye and adsorbents: (a)
1129 Electrostatic interactions, (b) dipole-dipole H-bonding interactions, (c) Yoshida Hbonding, and

1130 (d) n - π stacking interactions. (Reprinted with permission from Ref. (Sodkouieh et al., 2023).
1131 Copyright 2023 Springer).

1132 **Fig. 4.** Possible interaction mechanisms for lead(II) adsorption by a) wheat straw biochar and b)
1133 wheat straw hydrochar. (Reprinted with permission from Ref. (Nzediegwu et al., 2021).
1134 Copyright 2021 Elsevier).

1135 **Fig. 5.** Scheme of the possible mechanism for tetracycline TC adsorption on KMnO_4 activated
1136 wheat straw biochar Mn-BC. (Reprinted with permission from Ref. (Huang et al., 2023).
1137 Copyright 2023 Elsevier).

1138 **Table Captions**

1139 **Table 1.** Lignocellulosic content of various wheat residues.

1140 **Table 2.** Maximum uptakes and the best applied isotherm/kinetic model of synthetic dyes
1141 adsorption onto various wheat residues-based adsorbents.

1142 **Table 3.** Maximum uptakes and the best applied isotherm/kinetic model of heavy metal ions
1143 adsorption onto various wheat residues-based adsorbents.

1144 **Table 4.** Maximum uptakes and the best applied isotherm/kinetic model of other contaminants
1145 adsorption onto various wheat residues-based adsorbents.

1146 **Table 5.** Regeneration results of wheat residues- based adsorbents loaded with different
1147 contaminants.

Table 1. Lignocellulosic content of various wheat residues.

Wheat residue	Cellulose (%)	Hemicellulose (%)	Lignin (%)	Reference
Wheat straw	45.32	19.89	12.49	(Chen et al., 2020)
Wheat straw	43.10	29.02	19.31	(Pirbazari et al., 2016)
Wheat husk	37.00	16.54	17.20	(Franco et al., 2021)
Wheat husk	36.0	18.0	16.0	(Mirjalili et al., 2011)
Wheat bran	17.30	51.80	10.70	(Fricler et al., 2023)
Wheat bran	32.1	29.2	16.4	(Zhang et al., 2018)
Wheat stalk	37.48	26.02	14.75	(Kumar & Prakash, 2023)
Wheat stalk	43.5	34.4	18.3	(Li et al., 2018)

Table 2. Maximum uptakes and the best applied isotherm/kinetic model of synthetic dyes adsorption onto various wheat residues-based adsorbents.

Adsorbent	Synthetic dye	q_{\max} (mg/g)	Isotherm	Kinetic	Reference
Citric acid modified WS	Methylene blue	450.0	Langmuir, Freundlich	PSO	(Han et al., 2010)
NaOH/Fe ₃ O ₄ modified WS	Methylene blue	1374.6	Freundlich	PFO	(Pirbazari et al., 2014)
Phytic acid modified WS	Methylene blue	220.9	Langmuir	PSO	(You et al., 2016)
Polymer modified WS	Methylene blue	115	-	PSO	(Lin et al., 2017)
Perchloric acid modified WH	Methylene blue	4.23	Langmuir	PSO	(Banerjee et al., 2014)
Raw WS	Methylene blue	45.9	Langmuir	-	(Ben'ko & Lunin, 2018)
Biomass fly ash/WS biochar composite	Methylene blue	854.75	Freundlich	PSO	(Li et al., 2023)
NaOH/monochloroacetic acid modified WS	Methylene blue	191.427	Langmuir	PSO	(Sodkouieh et al., 2023)
NaOH modified WS	Methylene blue	131.123	Langmuir	PSO	(Sodkouieh et al., 2023)
Cinnamic acid modified WH biochar	Methylene blue	427.35	Langmuir	PSO	(Habiba et al., 2022)
NaOH modified WS	Methylene blue	85.470	Langmuir	PSO	(Laidani et al., 2019)
Raw WS	Methylene blue	172.414	Langmuir	PSO	(Pirbazari et al., 2016)
Tartaric acid modified WB	Methylene blue	25.18	Langmuir, Freundlich	PSO	(Yao et al., 2012)
WS biochar	Malachite green	1449.4	Langmuir	PSO	(Yang et al., 2019)
WB biochar	Malachite green	1301.9	Langmuir	PSO	(Yang et al., 2019)
WB/H ₂ SO ₄ carbon	Malachite green	69.0	Langmuir	PSO	(Mukwa et al., 2017)
NaOH/carbon disulphite modified WB carbon	Malachite green	112.9	Langmuir	PSO	(Dhami & Homagai, 2020)
Raw WH	Malachite green	2.344	Langmuir	PSO	(Mohamed et al., 2019)
Raw WB	Methyl orange	19.85	-	PSO, PFO	(Alzaydien, 2015)
Quaternary ammonium modified WS	Methyl orange	350.9	Langmuir	PSO	(Zhang et al., 2012)
Amine/NaOH modified WS	Methyl orange	304.2	Langmuir, Sips, Redlich-Peterson	PSO	(Aliabadi et al., 2018)
CTAB surfactant modified WS	Congo red	71.2	Langmuir	PFO	(Zhang et al., 2014a)
Raw WH	Congo red	38.61	Langmuir	PSO	(Sabah & Alwared, 2019)
Raw WB	Crystal violet	116.94	Langmuir	PSO	(Haq et al., 2021)
Gemini surfactant modified WB	Acid red 18	67.24	Langmuir	PSO	(Zhang et al., 2017)
Gemini surfactant modified WB	Acid orange 7	85.12	Langmuir	PSO	(Zhang et al., 2017)
Sodium bicarbonate modified WB	Acid orange 7	92.64	Freundlich	PSO	(Mohammadi et al., 2021)
Gemini surfactant modified WB	Acid black 1	83.51	Langmuir	PSO	(Zhang et al., 2017)
Polymer modified WS	Orange II	506	-	PSO	(Lin et al., 2017)
CTAB surfactant modified WB	Acid red 18	65.41	Langmuir	PSO	(Zhang et al., 2018b)

FeCl ₃ modified WS hydrochar	Rhodamine B	80	Langmuir, Freundlich	PSO	(Kohzadi et al., 2023)
MgCl ₂ /NaOH modified WS biochar	Directly frozen yellow	205.5	Langmuir	-	(Zhang et al., 2014b)
HClO ₄ modified WH	Reactive yellow 15	5.3561	Langmuir	-	(Mirjalili et al., 2011)
Quaternary ammonium modified WS	Acid green 25	952.3	Langmuir	PSO	(Zhang et al., 2012)
Raw WS	Basic yellow 21	71.43	Temkin	PSO	(Hassanein & Koumanova, 2010)
Raw WB	Coomassie brilliant blue	6.410	Langmuir	PSO	(Ata et al., 2012)
WH (soaked in HNO ₃)	Reactive blue 19	2.336	Langmuir, Freundlich	-	(Vasu et al., 2019)
WH (soaked in HNO ₃)	Reactive red 195	2.100	Langmuir, Freundlich	-	(Vasu et al., 2019)
Perchloric acid modified WH	Acid orange 10	31.29	Freundlich	PSO	(Banerjee et al., 2015)

WS: wheat straw, WB: wheat bran, WH: wheat husk, PFO: pseudo-first order, PSO: pseudo-second order

Table 3. Maximum uptakes and the best applied isotherm/kinetic model of heavy metal ions adsorption onto various wheat residues-based adsorbents.

Adsorbent	Heavy metal	q_{\max} (mg/g)	Isotherm	Kinetic	Reference
WS biochar	Pb(II)	251.71	Langmuir	PSO	(Qi et al., 2023)
WS biochar	Pb(II)	17.95	Langmuir	PSO	(Wang et al., 2022)
Amino modified WS biochar	Pb(II)	46.84	Langmuir	PSO	(Wang et al., 2022)
WS biochar	Pb(II)	134.68	-	-	(Cao et al., 2019a)
Raw WS	Pb(II)	46.33	-	-	(Cao et al., 2019a)
Acetic acid modified WB	Pb(II)	13.31	Langmuir	PSO	(Xing et al., 2013)
WS biochar	Pb(II)	80.19	Langmuir	IPD	(Zhang et al., 2022)
Raw WB	Pb(II)	1.667	Langmuir, Freundlich	PSO	(Ogata et al., 2014)
WS/ZnCl ₂ biochar	Pb(II)	149.701	Langmuir	PSO	(Mu et al., 2018a)
WS biochar	Pb(II)	157.95	-	-	(Cao et al., 2019b)
WS/steam activated biochar	Pb(II)	125.0	Freundlich	PSO	(Kwak et al., 2019)
WS biochar	Pb(II)	109.0	Freundlich	PSO	(Kwak et al., 2019)
WB/NaOH activated carbon	Pb(II)	448.2	Langmuir	PSO	(Zhang et al., 2020a)
WS biochar	Pb(II)	68.44	Temkin, Freundlich	PSO	(Nzediegwu et al., 2021)
WS hydrochar	Pb(II)	9.94	Freundlich	PSO	(Nzediegwu et al., 2021)
Magnetic Fe ₃ O ₄ WL biochar	Pb(II)	179.85	Langmuir, Freundlich	PSO	(Li et al., 2020)
WL biochar	Pb(II)	160.39	Langmuir, Freundlich	PSO	(Li et al., 2020)
WS biochar	Pb(II)	134.68	-	-	(Cao et al., 2019b)
Raw WS	Pb(II)	46.33	-	-	(Cao et al., 2019b)
Magnetic Fe ₂ O ₃ WS biochar	Pb(II)	196.91	Freundlich	PSO	(Zhao et al., 2019)
Raw WS	Pb(II)	0.38	Langmuir	PSO	(Anis et al., 2013)
WS biochar	Pb(II)	35.95	-	PSO, Elovich	(Wang et al., 2011)
Lactic acid modified WS	Pb(II)	51.49	Langmuir	PSO	(Mu et al., 2018b)
Magnetic Fe ₃ O ₄ modified WS	Pb(II)	50.76	Langmuir	PSO	(Haghighat & Ameri, 2016)
Raw WS	Pb(II)	41.15	Langmuir	PSO	(Haghighat & Ameri, 2016)
Raw WS	Pb(II)	41.60	Langmuir	-	(Ameri et al., 2014)
Amine crosslinked WS	Cr(VI)	295.34	Langmuir	-	(Xu et al., 2011a)
Diethylenetriamine modified WS	Cr(VI)	322.58	Freundlich	PSO	(Chen et al., 2010)
WS carbon	Cr(VI)	21.34	Freundlich	PSO	(Wang et al., 2010)
Raw WS	Cr(VI)	125.6	Langmuir	PSO	(Chen et al., 2020a)

Tartaric acid modified WB	Cr(VI)	23.918	Freundlich	-	(Kaya et al., 2014)
Raw WB	Cr(VI)	1.206	Freundlich	-	(Kaya et al., 2014)
WS biochar	Cr(VI)	97%	-	PSO	(Wang et al., 2023a)
WS carbon	Cr(VI)	21.34	Freundlich	PSO	(Wang et al., 2010)
Amphoteric (amino/acid) WS	Cr(VI)	227.3	Langmuir	-	(Zhong et al., 2013)
Raw WS	Cr(VI)	30.94	Langmuir	-	(Zhong et al., 2013)
Calcined WB	Cr(VI)	29.3	Freundlich	PSO	(Ogata et al., 2020)
Raw WB	Cr(VI)	4.2	Freundlich	PSO	(Ogata et al., 2020)
KOH activated WS biochar	Cr(VI)	96.082	Freundlich	PSO, Elovich	(Jamil et al., 2023)
WS biochar	Cr(VI)	42.0	Langmuir	PSO	(Ali et al., 2020)
WL biochar	Cr(VI)	-	-	PFO	(Liu et al., 2022a)
Raw WS	Cr(III)	68.9	Langmuir	PSO	(Chen et al., 2020a)
Polyethylenimine modified WS	Cu(II)	54.4	Freundlich	Elovich	(Dong et al., 2019)
Citric acid modified WS	Cu(II)	55.42	Langmuir, Freundlich	PSO	(Han et al., 2010)
NaOH modified WS	Cu(II)	10.680	Freundlich	PSO	(Guo et al., 2016)
Raw WS	Cu(II)	10.238	Freundlich	PSO	(Guo et al., 2016)
WS biochar	Cu(II)	578.13	Langmuir	PSO	(Qi et al., 2023)
Iron K ₂ FeO ₄ modified WL biochar	Cu(II)	46.849	Langmuir	PSO	(Yan et al., 2022)
Raw WS	Cu(II)	4.3	Langmuir	PSO	(Gorgievski et al., 2013)
Amphoteric (amino/acid) WS	Cu(II)	73.53	Langmuir	-	(Zhong et al., 2013)
Raw WS	Cu(II)	16.01	Langmuir	-	(Zhong et al., 2013)
Raw WS	Cu(II)	0.58	Langmuir	PSO	(Anis et al., 2013)
Raw WH	Cu(II)	3.97	Freundlich	Elovich	(Liu et al., 2012)
Amino modified WS biochar	Cu(II)	19.79	Langmuir	PSO	(Wang et al., 2022)
WS biochar	Cu(II)	8.86	Langmuir	PSO	(Wang et al., 2022)
Nano-chlorapatite modified WH biochar	Cd(II)	183.486	Langmuir	PSO	(Yuan et al., 2023)
WH biochar	Cd(II)	4.209	Langmuir	PSO	(Yuan et al., 2023)
Raw WB	Cd(II)	0.667	Langmuir, Freundlich	PSO	(Ogata et al., 2014)
WS biochar	Cd(II)	215.55	Langmuir	PSO	(Qi et al., 2023)
WS biochar	Cd(II)	32.57	Langmuir	PSO	(Bogusz et al., 2017)
Sulfur CS ₂ modified WS biochar	Cd(II)	41.376	Langmuir	PSO	(Chen et al., 2020b)
WS biochar	Cd(II)	33.410	Langmuir	PSO	(Chen et al., 2020b)
Raw WS	Cd(II)	8.577	Langmuir, Freundlich	-	(Coelho et al., 2016)
Urea modified WS	Cd(II)	39.22	Langmuir	PSO	(Farooq et al., 2011)

Raw WS	Cd(II)	4.25	Freundlich	PSO	(Farooq et al., 2011)
Raw WS	Cd(II)	31.546	Langmuir	PSO	(Dutta et al., 2016)
Amino modified WS biochar	Cd(II)	10.37	Langmuir	PSO	(Wang et al., 2022)
WS biochar	Cd(II)	4.74	Langmuir	PSO	(Wang et al., 2022)
Ethanol/NaOH modified WS	Cd(II)	14.27	Langmuir, Temkin	PSO	(Wu et al., 2019)
WS biochar	Ni(II)	25.06	Freundlich	-	(Shen et al., 2017)
WS biochar	Ni(II)	17.67	Langmuir	PSO	(Bogusz et al., 2017)
Raw WS	Ni(II)	2.5	Langmuir	PSO	(Gorgievski et al., 2013)
Raw WS	Zn(II)	3.6	Langmuir	PSO	(Gorgievski et al., 2013)
WS biochar	Hg(II)	5.85	Langmuir	PSO	(Zhang et al., 2018c)
Fe ₃ O ₄ magnetic WS	As(V)	8.062	Langmuir	-	(Tian et al., 2011)
Fe ₃ O ₄ magnetic WS	As(III)	3.898	Langmuir	-	(Tian et al., 2011)
Calcined WB	Pt(IV)	22.0	Langmuir, Freundlich	PSO	(Ogata et al., 2022)
Raw WB	Pt(IV)	6.74	Langmuir, Freundlich	PSO	(Ogata et al., 2022)
WB-titanium oxide composite	Se(VI)	3.79	Langmuir	PSO	(Li et al., 2021)

WS: wheat straw, WB: wheat bran, WH: wheat husk, WL: wheat stalk, PFO: pseudo-first order, PSO: pseudo-second order, IPD: intraparticle diffusion

Table 4. Maximum uptakes and the best applied isotherm/kinetic model of other contaminants adsorption onto various wheat residues-based adsorbents.

Adsorbent	Pollutant	q_{\max} (mg/g)	Isotherm	Kinetic	Reference
KMnO ₄ /KOH modified WS biochar	Tetracycline	584.19	Langmuir	PSO	(Xu et al., 2022)
Lignin modified WL biochar	Tetracycline	31.48	Langmuir	PSO	(Xiang et al., 2022)
Zirconium modified WS	Tetracycline	80.6	-	PSO	(Wang et al., 2021)
MOFs/WS biochar composite	Tetracycline	854.75	Freundlich	PSO	(Li et al., 2023)
KOH activated WS biochar	Tetracycline	222.2	Langmuir, Freundlich, Temkin	PSO	(Liu et al., 2022b)
WS biochar	Tetracycline	75.76	Langmuir, Freundlich, Temkin	PSO	(Liu et al., 2022b)
Montmorillonite- WS biochar composite	Norfloracin	25.53	Langmuir	-	(Zhang et al., 2018a)
WS biochar	Norfloracin	10.58	Langmuir	-	(Zhang et al., 2018a)
Iron (K ₂ FeO ₄) modified WL biochar	Sulfadiazine	45.431	Freundlich	PSO	(Yan et al., 2022)
H ₂ SO ₄ modified WB	Tylosin	61.61	Temkin, Langmuir	PSO	(Sarrai et al., 2022)
Raw WS	Cefradine	39.5	Freundlich	-	(Deng et al., 2019)
WS biochar	Sulfamethazine	18.282	Langmuir, Freundlich	-	(Yang et al., 2020)
Amine modified WS	Nitrate	77.0	Freundlich	-	(Shi et al., 2022b)
Ca-La-trimethylamine modified WS	Nitrate	72.89	Langmuir	PSO	(Zhang et al., 2023)
Raw WS	Nitrate	94.25	Langmuir	-	(Shahaji et al., 2023)
Silane/octane modified WS	Nitrate	47.95	Langmuir	GO	(Mehdinejadani et al., 2019)
KMnO ₄ activated WS biochar	Nitrate	107.77	Freundlich	PSO	(Huang et al., 2023)
WS biochar	Nitrate	32.12	Freundlich	PSO	(Huang et al., 2023)
Amine crosslinked WS	Phosphate	162.40	Langmuir	-	(Xu et al., 2011a)
Ca-La-trimethylamine modified WS	Phosphate	86.97	Langmuir	PSO	(Zhang et al., 2023)
Mg/Fe doped WS biochar	Phosphate	179.21	Langmuir, Freundlich	PSO, PFO	(Wang et al., 2023b)
Amine crosslinked WS	Phosphate	60.61	Langmuir	-	(Xu et al., 2011b)
Dimethyl diallyl ammonium chloride modified WS	Phosphate	8.43	Freundlich	PSO	(Ma et al., 2011)
Dimethyl diallyl ammonium chloride modified WS	Ammonium	85.47	Langmuir, Freundlich	PSO	(Ma et al., 2011)
FeCl ₃ /HCl modified WS biochar	Ammonium	99.6	Langmuir	PSO, PFO	(Wang et al., 2020)
WS biochar	Ammonium	85.1	Langmuir	PSO, PFO	(Wang et al., 2020)
WS biochar	Ammonium	2.08	Redlich-Peterson	PSO	(Yang et al., 2018)

MgCl ₂ /CeCl ₂ modified WS biochar	Phosphorus	13.0	Langmuir	PSO	(Pan et al., 2023)
Triethylamine modified WS	Perchlorate	119.0	Langmuir	PSO	(Tan et al., 2012)
Raw WS	Fluoride	1.93	Freundlich	PSO	(Yadav et al., 2013)
Raw WS	Sodium ion	48.08	Langmuir	PSO	(Rasouli et al., 2020)
H ₂ SO ₄ modified WH	2,4-D herbicide	140.2	Liu	Avrami	(Franco et al., 2021)
KOH modified WS carbon	2,4-D herbicide	1.015	Langmuir	-	(Tefera & Tulu, 2021)
LiNO ₃ -functionalized WS biochar	Atrazine	272.07	Freundlich	IPD	(Yang et al., 2017)
WS biochar	Atrazine	61.37	Langmuir	IPD	(Yang et al., 2017)
WS biochar	Atrazine	20.161	Langmuir	PSO	(Wang et al., 2016)
WS/H ₃ PO ₄ activated carbon	Phenol	285.71	-	PSO	(Shou & Qiu, 2016)
ZnCl ₂ modified WS biochar	4-Chlorophenol	111.02	Langmuir, Freundlich	PSO	(Shen et al., 2021)
ZnCl ₂ activated WS hydrochar	Bisphenol A	909.1	Langmuir	PSO	(Shi et al., 2022a)
WS biochar	Bisphenol A	625.0	Langmuir	PSO	(Shi et al., 2022a)
WS/KOH activated carbon	Diphenolic acid	264.90	Langmuir	PSO	(Alrowais et al., 2023)

WS: wheat straw, WB: wheat bran, WH: wheat husk, WL: wheat stalk, PFO: pseudo-first order, PSO: pseudo-second order, IPD: intraparticle diffusion, GO: general order

Table 5. Regeneration results of wheat residues- based adsorbents loaded with different contaminants.

Adsorbent	Pollutant	Eluent	No. of cycles	Drop in capacity or removal %	Ref.
Montmorillonite-WS biochar composite	Norfloxacin	Methanol	5	86.8-86.5%	(Zhang et al., 2018a)
Raw WB	Pt(IV)	NaOH, HNO ₃ , HCl (0.5 or 1M)	1	59.3 or 64.5%, 56.4 or 59.3%, 59.9 or 64.0%	(Ogata et al., 2022)
Polyethylenimine modified WS	Cu(II)	0.1M HCl	3	<70%->60%	(Dong et al., 2019)
Amine modified WS	Nitrate	HCl, NaCl, NaOH (0.1M)	1	87.2, 69.1, 93.6%	(Shi et al., 2022b)
Zirconium modified WS	Tetracycline	0.1 M HCl	3	60.3-45.2%	(Wang et al., 2021)
NaOH/Fe ₃ O ₄ modified WS	Methylene blue	Deionized water	1	9.0-12.0%	(Pirbazari et al., 2014)
Fe ₃ O ₄ magnetic WS	As(V)	0.1 M NaOH	10	100-91%	(Tian et al., 2011)
Phytic acid modified WS	Methylene blue	0.1M HCl	4	93.4-68.5%	(You et al., 2016)
ZnCl ₂ activated WS hydrochar	Bisphenol A	Ethanol	5	98.3-82.8%	(Shi et al., 2022a)
Ca-La-trimethylamine modified WS	Nitrate	10% NaCl+NaOH	9	46.88-40.0 mg/g	(Zhang et al., 2023)
Ca-La-trimethylamine modified WS	Phosphate	10% NaCl+NaOH	9	79.8-70.2 mg/g	(Zhang et al., 2023)
CTAB surfactant modified WS	Congo red	0.1 M NaOH	3	78.4-54.1%	(Zhang et al., 2014a)
Raw WB	Molybdenum	1 or 0.1M NaOH	1	95.0 or 94.2%	(Ogata et al., 2018)
ZnCl ₂ modified WS biochar	4-Chlorophenol	DI water+ peroxydisulfate	4	94.0-81.67%	(Shen et al., 2021)
H ₂ SO ₄ modified WH	2,4-D herbicide	0.5 M NaOH	5	47.57-45.39%	(Franco et al., 2021)
CTAB surfactant modified WB	Acid red 18	Ethanol (75vol%)	1	78.68%	(Zhang et al., 2018b)
FeCl ₃ modified WS hydrochar	Rhodamin B	H ₂ O (pH 6)	3	4.55-2.55%	(Kohzadi et al., 2023)
Raw WB	Cd(II)	0.01M HCl, 0.01M HNO ₃	4	17.9-4.2 mg/g, 17.9-4.3 mg/g	(Ogata et al., 2014)
Raw WB	Pb(II)	0.01M HCl, 0.01M HNO ₃	4	27.5-14.9 mg/g, 27.5-13.3 mg/g	(Ogata et al., 2014)
Raw WS	Cr(VI)	1M KOH	10	80.625-76.875 mg/g	(Chen et al., 2020a)
Raw WS	Cr(III)	0.1M HNO ₃	10	46.875-44.0 mg/g	(Chen et al., 2020a)
WS biochar	Hg(II)	0.01M HNO ₃	1	31.5% or 1.03 mg/g	(Zhang et al., 2018c)
Raw WS	Sodium ion	0.1 M HCl	5	89.89-52.38%	(Rasouli et al., 2020)

MgCl ₂ /NaOH modified WS biochar	Directly frozen yellow	0.01M NaOH	1	55.2%	(Zhang et al., 2014b)
Tartaric acid modified WB	Cr(VI)	0.5 M HCl	1	80% (pH 7), 99% (pH 14)	(Kaya et al., 2014)
Silane/octane modified WS	Nitrate	NaCl sat. solution	5	85.0-82.6%	(Mehdinejadani et al., 2019)
WS biochar	Pb(II), Cd(II), Cu(II)	2M HCl	1	56.22, 96.07, 76.17%	(Qi et al., 2023)
WS biochar	Cd(II)	HCl, HNO ₃	1	70.0, 80.0%	(Bogusz et al., 2017)
WS biochar	Ni(II)	HCl, HNO ₃	1	99.0, 99.0%	(Bogusz et al., 2017)
WB/NaOH activated carbon	Pb(II)	0.2M HCl	4	99.0-94.9%	(Zhang et al., 2020a)
KMnO ₄ activated WS biochar	Tetracycline	0.5 M NaOH, Methanol, Thermal	3	90.67-80.72%, 89.62-40.17%, 90.90-25.71%	(Huang et al., 2023)
WS biochar	Pb(II)	0.1 M HCl, Deionized H ₂ O	1	92.0, 0.4%	(Nzediegwu et al., 2021)
WS hydrochar	Pb(II)	0.1 M HCl, Deionized H ₂ O	1	100.0, 15.0%	(Nzediegwu et al., 2021)
Iron K ₂ FeO ₄ modified WL biochar	Cu(II), Sulfadiazine	0.1 M NaOH	3	18-14.375%, 31.67-24.9%	(Yan et al., 2022)
Raw WS	Cd(II), Cu(II), Pb(II)	0.01 M NaNO ₃	1	8.7, 17.9, 5.0%	(Coelho et al., 2016)
Quaternary ammonium modified WS	Methyl orange, Acid green 25	Deionized water	1	22.2, 14.7%	(Zhang et al., 2012)
Magnetic WS biochar	Pb(II)	HCl	5	32.4-41.7 mg/g	(Zhao et al., 2019)
Calcined WB	Cr(VI)	1M NaOH	5	49-48%	(Ogata et al., 2020)
KOH activated WS biochar	Cr(VI)	1M NaOH	4	98.33-48.98%	(Jamil et al., 2023)
NaOH modified WS	Methylene blue	0.01M HCl, 0.01M NaCl	5	75.4%, 17.8%	(Sodkouieh et al., 2023)
NaOH/monochloroacetic acid modified WS	Methylene blue	0.01M HCl 0.01M NaCl	5	84.8%, 24.6%	(Sodkouieh et al., 2023)
Amine/NaOH modified WS	Methyl orange	Neutral distilled water	1	2%	(Aliabadi et al., 2018)
Amine/NaOH modified WS	Methyl orange	0.1M HCl	1	10%	(Aliabadi et al., 2018)
WS biochar	Atrazine	Methanol	3	31.2-22.3 mg/g	(Wang et al., 2016)
Perchloric acid modified WH	Acid orange 10	0.1M NaOH	3	>80%-<60%	(Banerjee et al., 2016)

WS: wheat straw, WB: wheat bran, WH: wheat husk, WL: wheat stalk

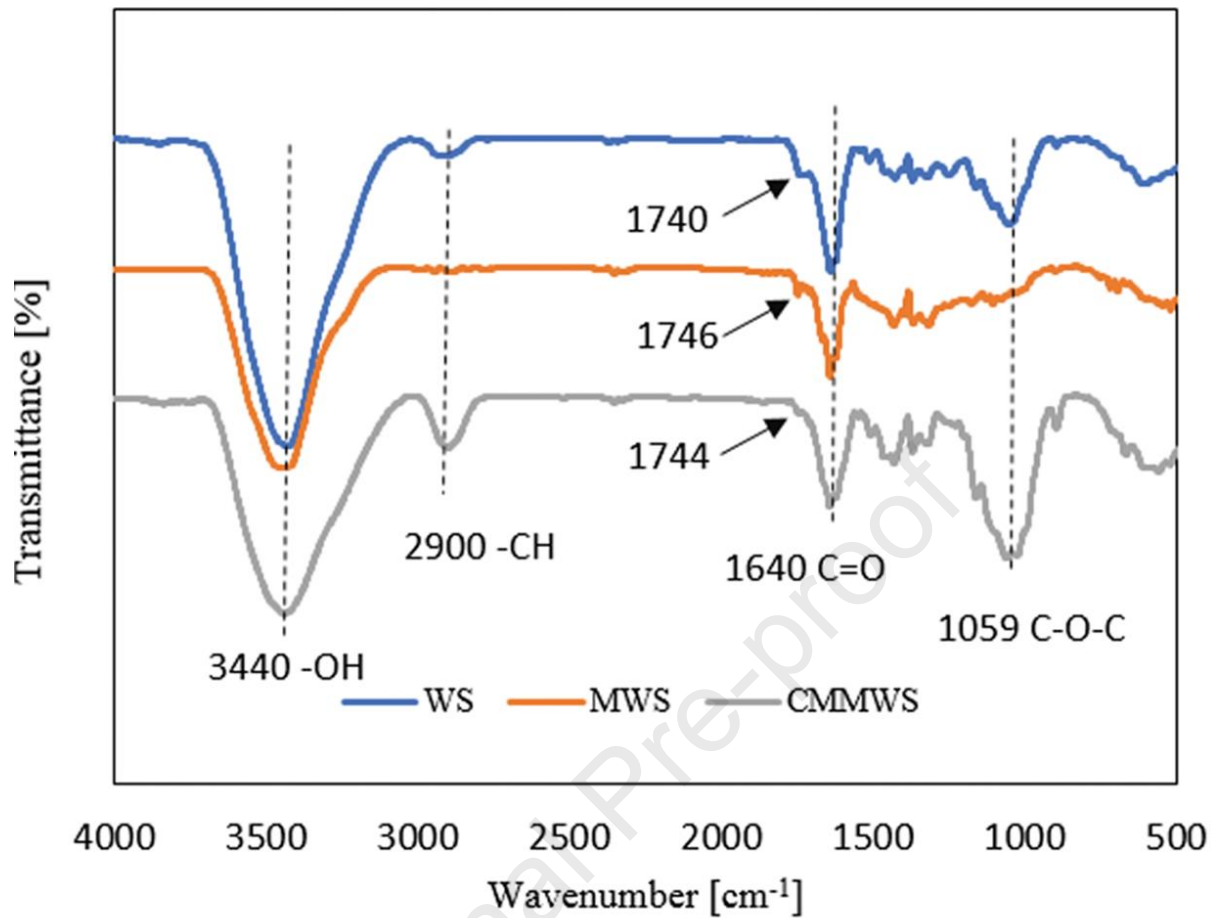


Fig. 1. FTIR spectra of raw WS, NaOH modified MWS, and NaOH/monochloroacetic acid modified CMMWS wheat straws. (Reprinted with permission from Ref. (Sodkouieh et al., 2023). Copyright 2023 Springer).

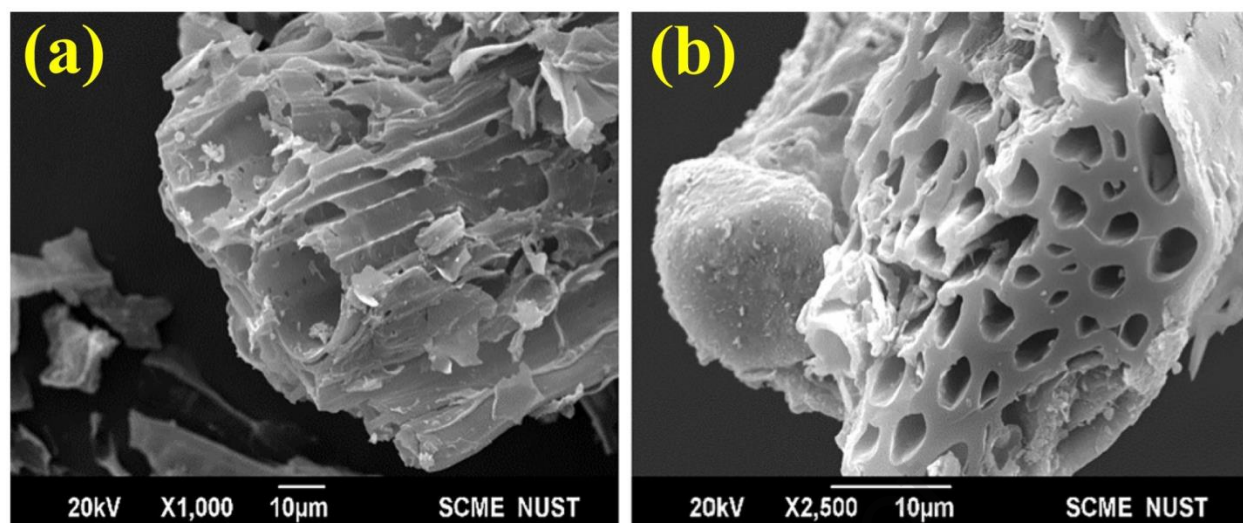


Fig. 2. SEM images of (a) wheat straw biochar WSBC (b) KOH activated biochar WSKOH_{dry} 1:3. (Reprinted with permission from Ref. (Jamil et al., 2023). Copyright 2023 Elsevier).

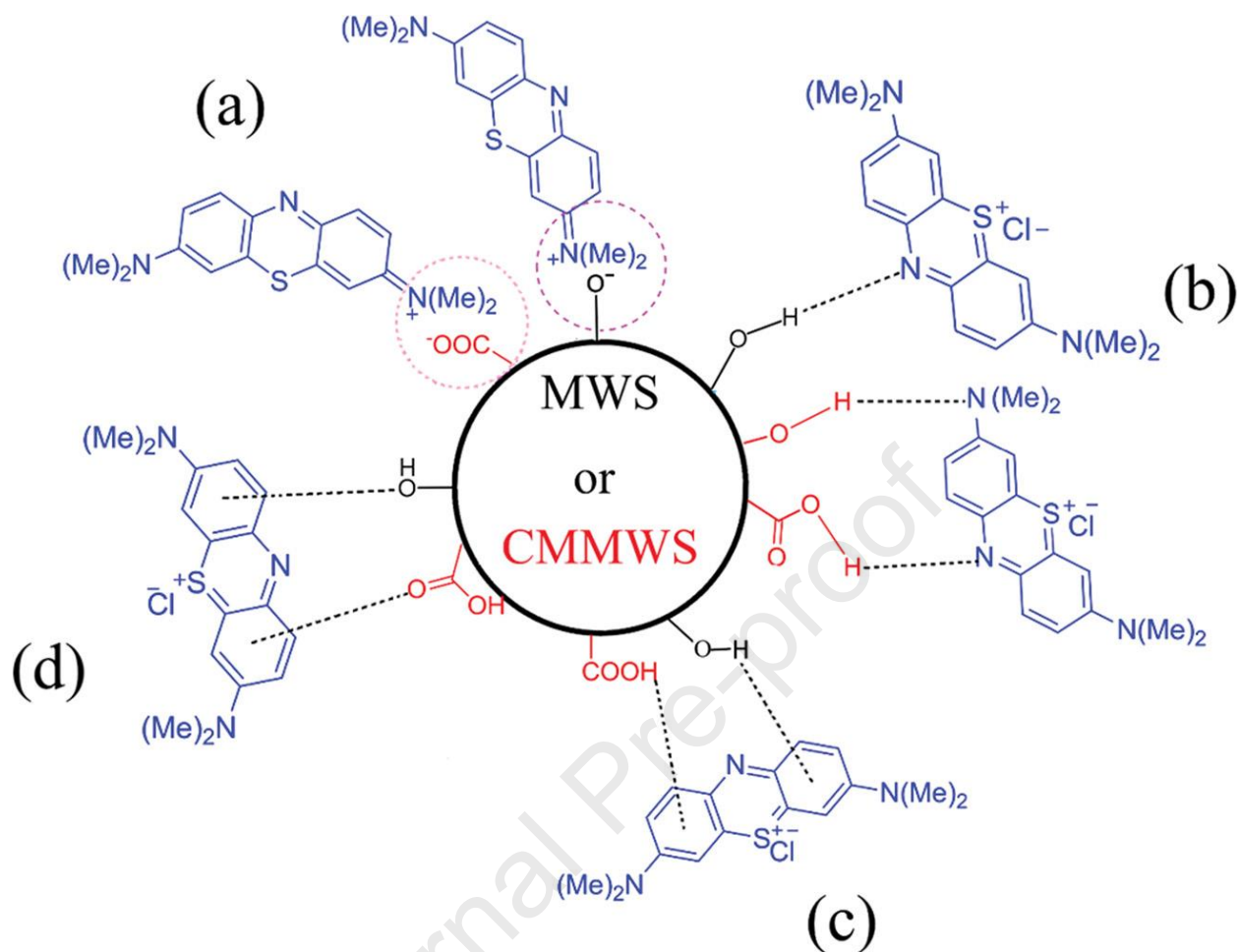


Fig. 3. Illustration of the potential mechanism of interaction between MB dye and adsorbents: (a) Electrostatic interactions, (b) dipole-dipole H-bonding interactions, (c) Yoshida Hbonding, and (d) n- π stacking interactions. (Reprinted with permission from Ref. (Sodkouieh et al., 2023). Copyright 2023 Springer).

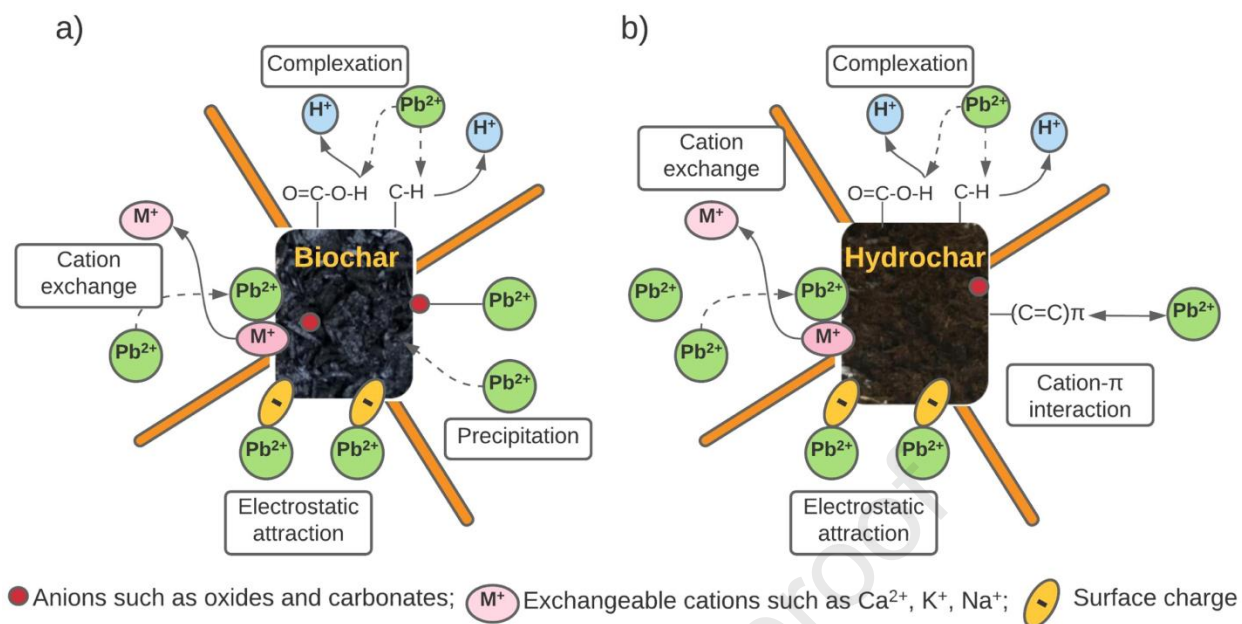


Fig. 4. Possible interaction mechanisms for lead(II) adsorption by a) wheat straw biochar and b) wheat straw hydrochar. (Reprinted with permission from Ref. (Nzediegwu et al., 2021).

Copyright 2021 Elsevier).

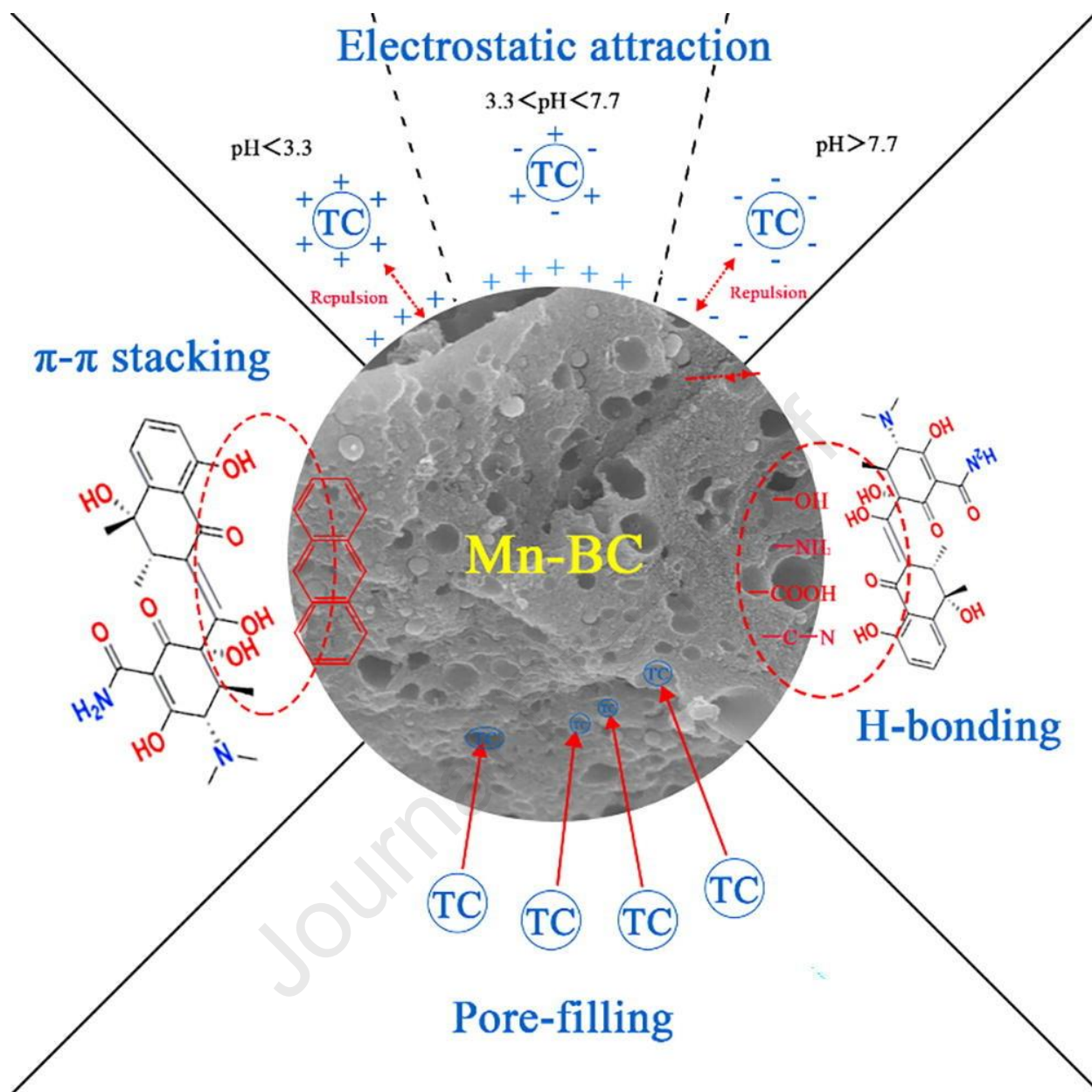


Fig. 5. Scheme of the possible mechanism for tetracycline TC adsorption on KMnO_4 activated wheat straw biochar Mn-BC. (Reprinted with permission from Ref. (Huang et al., 2023).

Copyright 2023 Elsevier).

Declaration of interests

The authors declare that they have no known competing financial interests or personal relationships that could have appeared to influence the work reported in this paper.

The authors declare the following financial interests/personal relationships which may be considered as potential competing interests:

Journal Pre-proof